

Expert-Guided Inverse Optimization for Convex Constraint Inference

Houra Mahmoudzadeh*

Department of Management Science and Engineering, University of Waterloo, ON, Canada. houra.mahmoudzadeh@uwaterloo.ca

Kimia Ghobadi*

Malone Center for Engineering in Healthcare, Center for Systems Science and Engineering, Department of Civil and Systems Engineering, Johns Hopkins University, Baltimore, MD, USA. kimia@jhu.edu

Abstract. Conventional inverse optimization inputs a solution and finds the parameters of an optimization model that render a given solution optimal. The literature mostly focuses on inferring the objective function in linear problems when accepted solutions are provided as input. In this paper, we propose an inverse optimization model that inputs several accepted and rejected solutions and recovers the underlying convex optimization model that can be used to generate such solutions. The novelty of our model is two-fold: First, we focus on inferring the parameters of the underlying convex feasible region. Second, the proposed model learns the convex constraint set from a set of past observations that are either accepted or rejected by an expert. The resulting inverse model is a mixed-integer nonlinear problem that is complex to solve. To mitigate the inverse problem complexity, we employ variational inequalities and the theoretical properties of the solutions to derive a reduced formulation that retains the complexity of its forward counterpart. Using realistic breast cancer patient data, we demonstrate that our inverse model can utilize a subset of past accepted and rejected treatment plans to infer clinical criteria that can lead to nearly guaranteed acceptable treatment plans for future patients.

Key words: inverse optimization, convex constraint inference, radiation therapy.

1. Introduction

In the era of big data, learning from past expert decisions and their corresponding outcomes, whether good or bad, provides an invaluable opportunity for improving future decision-making processes. While there is considerable momentum to learn from data through artificial intelligence, machine learning, and statistics, the field of operations research has not been using this valuable resource to its full potential in learning from past decisions to inform future decision-making processes. One of the emerging methodologies that can benefit from this abundance of data is inverse optimization ([Ahuja and Orlin 2001](#)).

A regular (forward) optimization problem models a system and determines an optimal solution that represents a decision for the system. On the contrary, inverse optimization aims to recover the optimization model that made a set of given observed solutions (or decisions) optimal. For instance, in radiation therapy treatment planning for cancer patients, radiation oncologists make decisions on whether the quality of personalized plans generated through a treatment planning system is acceptable for each patient. In this case, an inverse model would be able to learn the implicit logic behind the oncologist’s decision-making process. Traditionally, the input to inverse models almost exclusively constitutes ‘good’ solutions that are optimal or near-optimal, regardless of feasibility. Little attention has been paid to learning from ‘bad’ solutions that must be avoided. In inverse optimization, learning from both ‘good’ and ‘bad’ observed solutions can provide invaluable information about the patterns, preferences, and restrictions of the underlying forward optimization model.

The inverse optimization literature largely focuses on inferring the objective coefficients of a forward model. The parameters often denote the utility or preferences of a decision-maker, when feasibility conditions are known. Very little attention has been paid to recovering the constraints. There are three fundamental differences between recovering an objective function of an optimization problem when the feasible set is known and recovering the feasible region itself. Firstly, when recovering the objective, an inverse model aims to satisfy optimality conditions for observed solutions (projections), regardless of their feasibility. On the contrary, when constraints are to be inferred, the focus shifts to satisfying feasibility conditions for the observed solutions while maintaining optimality conditions on a subset of observations that are optimal. This difference results in a mathematically-complex model that is harder to formulate and solve and has

* Both authors contributed equally to this manuscript.

therefore largely been ignored in the literature, particularly in the presence of unfavorable solutions. Secondly, when inferring constraints, any solution can be made optimal by inferring tailored constraints that render the observed solution optimal. Hence, traditional measures of (near) optimality that are used for objective coefficients, e.g., duality gap measures, are not applicable. Thirdly, while good and bad decisions have various interpretations and implications when recovering objective functions, in the context of recovering constraints, they can be viewed as solutions that are deemed accepted (feasible) and rejected (infeasible) by an expert, respectively, which guide the true shape of the underlying feasible region.

Inverse optimization is well-studied for inferring linear optimization models (Chan et al. 2023). This focus is mostly due to the tractability and existence of optimality guarantees in linear programming. In practice, however, nonlinear models are sometimes better suited for characterizing complex systems and capturing past solutions' attributes. The literature also largely focuses on inferring the utility function of decision-makers, which can be interpreted as the objective function of an optimization problem when the feasible region is known. Inferring the feasible region itself, on the contrary, has not received much attention, which may be attributed to the fact that inverse models for constraint inference are nonlinear, even when the forward problem is linear. For linear problems, there have been recent attempts for recovering the forward feasible region through inverse optimization (Chan and Kaw 2020, Ghobadi 2014), however, these studies do not generalize to nonlinear problems and assume all observations are acceptable, hence do not incorporate expert-guided rejected observations in constraint inference.

In radiation therapy treatment planning for cancer patients, a large pool of historical treatment plans exists that can be used in an inverse learning process. A plan is often designed to meet a set of pre-determined and often conflicting criteria, which are referred to as clinical guidelines. These guidelines may be too strict or too relaxed (sometimes simultaneously), and as a result, some plans that satisfy the original guidelines may be rejected by oncologists and some seemingly infeasible plans may be accepted. This application lends itself well to using inverse optimization for inferring the true underlying clinical guidelines for patient populations, which can lead to more efficient treatment planning and improved quality of treatment. In other words, the goal is to learn the parameters of an implicit optimization problem that can be solved to produce acceptable plans for future patients. While much attention has been paid to understanding the tradeoff balance in the objective of cancer treatment using inverse optimization, the problem of understanding the feasible region and constructing proper clinical guidelines remains under-explored. An incorrect guideline or constraint in the optimization model can lead to a significantly different feasible region and affect the possible optimal solutions that the objective function can achieve.

In this paper, we focus on recovering convex constraints of an optimization model through a novel inverse optimization framework. Our model inputs a set of past observed decisions, that are either accepted or rejected by a rational expert decision-maker, and uses it to infer the underlying optimization problem that makes them feasible or infeasible, respectively. We further propose a reformulation of our inverse optimization model using variational inequalities to mitigate its complexity and improve solvability. We demonstrate the merit of our framework using the problem of radiation therapy treatment planning for breast cancer patients where we impute the underlying convex constraints that represent the implicit guidelines that the expert decision-maker had in mind. The results can aid in standardizing clinical guidelines that can be used to produce acceptable plans, and hence, improving the efficiency of the planning process.

Given a (forward) optimization problem with a set of partially known parameters, inverse optimization inputs a set of given solution(s) and recovers the problem parameters (Ahuja and Orlin 2001). The input solution is often a single observation that is optimal (Ghate 2020b, Iyengar and Kang 2005) or near-optimal (Chan et al. 2014b, Naghavi et al. 2019) in which case the inverse model minimizes some measure of the optimality gap of the single input. Recently, with more focus on data-driven models, multiple noisy observations have also been considered as the input to inverse models (Aswani et al. 2018, Babier et al. 2021, Bertsimas et al. 2015a, Chan et al. 2019, Chow and Recker 2012, Esfahani et al. 2018, Gupta and Zhang 2023, Keshavarz et al. 2011, Troutt et al. 2008, 2006, Zhang and Liu 1999), in which case, not all of the input observations can be (near-)optimal, and some measure of the collective data is often optimized instead. Some studies also consider uncertainty in data that affect the inverse models (Ghobadi et al.

2018), or infer the structure of solutions to the inverse model instead of reporting a single inverse solution (Tavashloğlu et al. 2018). For a comprehensive review of inverse optimization, we refer the readers to the review paper by Chan et al. (2023).

Inverse optimization has been extensively considered for inferring linear optimization models. When the underlying forward optimization is assumed to be nonlinear, sufficient conditions for optimality of observations cannot be guaranteed unless the model falls under specific classes such as convex optimization for which Karush-Kuhn-Tucker (KKT) conditions are sufficient for optimality (Boyd and Vandenberghe 2004). Zhang and Xu (2010) recover the objective function for linearly-constrained convex separable models. Zhang and Zhang (2010) propose an inverse conic model that infers quadratic constraints and shows that it be efficiently solved using the dual of the obtained semi-definite programs. Keshavarz et al. (2011) consider general convex models and use past observations to recover the objective function parameters by minimizing the optimality errors in KKT conditions. Aswani et al. (2019) also propose an NP-hard inverse optimization model to recover parameters for convex optimization models with noisy data and provide a duality-based reformulation.

The current inverse optimization literature mainly focuses on inferring the objective function of the underlying forward problem (Chan et al. 2023). Constraint inference, on the contrary, has received little attention. Recovering the right-hand side of the constraint parameters alongside the objective parameters has been explored by Chow and Recker (2012), Dempe and Lohse (2006) and Černý and Hladík (2016). Similarly, Birge et al. (2017) recover the right-hand side parameters so that a given observation becomes optimal utilizing properties of the specific application and Dempe and Lohse (2006), Güler and Hamacher (2010), Saez-Gallego and Morales (2018) make a given observation optimal or near-optimal. Chan and Kaw (2020) perturb the nearest facet to make a given observation optimal and hence, find the left-hand side parameter of a linear constraint when the right-hand side parameters are known. Ghatrani and Ghate (2022) infer the unknown transitional probabilities in Markov Decision Processes which are part of the left-hand-side of the constraint set. Ghatrani and Ghate (2024) infer left-hand side constraint parameters of a semi-definite program. Aswani et al. (2019) and Gupta and Zhang (2023) write KKT conditions to infer full convex problems, but only test their models to infer the objective parameters, due to the complexity of constraint inference. Closest to our work is the study by Ghobadi and Mahmoudzadeh (2021) in which the full set of the constraint parameters is inferred in a linear model where the objective function and a set of feasible observations are given. Their method utilizes properties of linear optimization and does not generalize to convex constraints.

When imputing the objective function parameters in forward models with known feasible regions, infeasible observations (as near-optimal decision) have been considered by Ahmadi et al. (2020), Babier et al. (2021), Chan et al. (2022), and Shahmoradi and Lee (2021), among others. In these studies, infeasible and feasible observations are used in a similar manner to extract information about the utility function and provide objective parameter trade-offs in the forward problem (Ahmadi et al. 2020, Shahmoradi and Lee 2021). Outliers and irrelevant observations may also be removed from the data prior to the optimization or as part of it. When imputing constraint parameters, on the contrary, infeasible observations provide additional information to guide the shape of the underlying feasible region by signaling areas that must be made infeasible. To our knowledge, such undesired observations that must be avoided have not been explored in an inverse setting for constraint inference.

Inverse optimization has found a wide range of applications including energy (Birge et al. 2017, Brucker and Shakhlevich 2009, Fernández-Blanco et al. 2021), dietary recommendations (Ahmadi et al. 2022, 2020, Ghobadi et al. 2018, Shahmoradi and Lee 2021, 2022), finance (Li 2021, Roland et al. 2016, Yu et al. 2023), and healthcare systems (Chan et al. 2022), to name a few. In particular, radiation therapy treatment planning for cancer has been studied in the context of inverse optimization (Ajayi et al. 2022, Babier et al. 2018, 2020, Boutilier et al. 2015, Chan et al. 2022, Chan and Lee 2018, Chan et al. 2014b, Ghate 2020a, Goli et al. 2018, Lee et al. 2013). For instance, both Chan and Lee (2018) and Sayre and Ruan (2014) input accepted treatment plans to recover the appropriate weights for a given set of convex objectives using inverse optimization. Gebken and Peitz (2021) finds the objective weights for unconstrained problems using singular value decomposition. Personalization for different patient groups has been explored by Boutilier

et al. (2015) by recovering the utility functions appropriate to each group. Ajayi et al. (2022) employs inverse optimization for feature selection to identify a sparse set of clinical objectives for prostate cancer patients. These studies all focus on understanding the underlying tradeoffs between different objective terms in radiation therapy treatment plans and only use accepted treatment plans as an input to their inverse models, regardless of their feasibility with respect to the clinical guidelines. In Section 1.1, we present some of the challenges of finding acceptable treatment plans based on current clinical guidelines, which motivate the methodologies proposed in this paper.

1.1. Cancer Treatment Motivation

In 2023, there were an estimated 1.96 million new cancer cases diagnosed and 609,820 cancer deaths in the United States, and approximately 60% of them received radiation therapy as part of their treatment (American Cancer Society 2023). The radiation therapy treatment planning process is a time-consuming process that often involves manual planning by a treatment planner and/or oncologist. The input of the planning process is a medical image (e.g., CT, MRI) which includes contours that delineate the cancerous region (i.e., tumor) and the surrounding healthy organs at risk (OAR). The goal is to find the direction, shape, and intensity of radiation beams such that a set of clinical metrics on the tumor and the surrounding healthy organs is satisfied. In current practice, there are clinical guidelines on these radiation metrics. However, these guidelines are not universally agreed upon and often differ per institution. Additionally, adherence to these guidelines is at the discretion of oncologists.

Planners often try to find a treatment plan that meets these clinical guidelines and forward it to an oncologist who will, in turn, either accept or reject the plan. If the plan is rejected, the planner receives a set of instructions on which metrics to adjust. This iterative process can lead to unnecessary back and forth between the planner and the oncologist and may involve manual relaxation of the required clinical criteria. This process continues until the plan is accepted by the oncologist.

As we will show later in Section 4, most accepted treatment plans do not meet all the clinical guidelines simultaneously, typically because there are trade-offs between different metrics, and some radiation dose limits are too restrictive for some patients. This will lead to an increased back-and-forth between the planner and the oncologist. Conversely, sometimes the practically accepted plans follow much tighter constraints than the guidelines because the oncologists may believe that some guidelines are too relaxed and better plans are achievable. In mathematical programming terminology, the implicit (unknown) feasible region, based on which oncologists make an acceptance/rejection decision, often does not align with the feasibility/infeasibility of plans for the guidelines. A hypothetical schematic of accepted and rejected plans with respect to two metrics (Tumor dose and OAR dose) is shown in Figure 1(a). It can be seen that some points do not meet the guidelines but are accepted and others meet all guidelines but are rejected. There may be other complex criteria that capture the trade-off between the OAR dose and the tumor that oncologists consider when deciding on the acceptability of a treatment plan, as shown in 1(b). Understanding these trade-offs results in more practical and standardized guidelines that allow the planners to accurately represent the feasible region of the treatment optimization problem. Solving such an optimization problem that considers the learned guidelines can help planners produce acceptable treatment plans for future patients.

In the radiation therapy treatment planning problem, we demonstrate that our inverse framework can learn from both accepted and rejected plans and infer the true underlying criteria based on which the accept/reject decisions are made. Finding such constraints enables us to better understand the implicit logic of oncologists in approving or rejecting treatment plans. In doing so, we help both oncologists and planners by (i) standardizing the guidelines and care practices, (ii) generating more realistic criteria on the trade-offs between clinical metrics based on past observations as opposed to simple upper/lower bounds on individual metrics, (iii) improving the quality of the initial plans according to the oncologist’s opinion and hence, reducing the number of iterations between planners and oncologists, and (iv) improving the quality of the final plans by preventing low-quality solutions that otherwise satisfy the acceptability thresholds, especially for automated treatment planning methods that heavily rely on provided radiation thresholds and may result in infeasibility if clinical thresholds are not personalized.

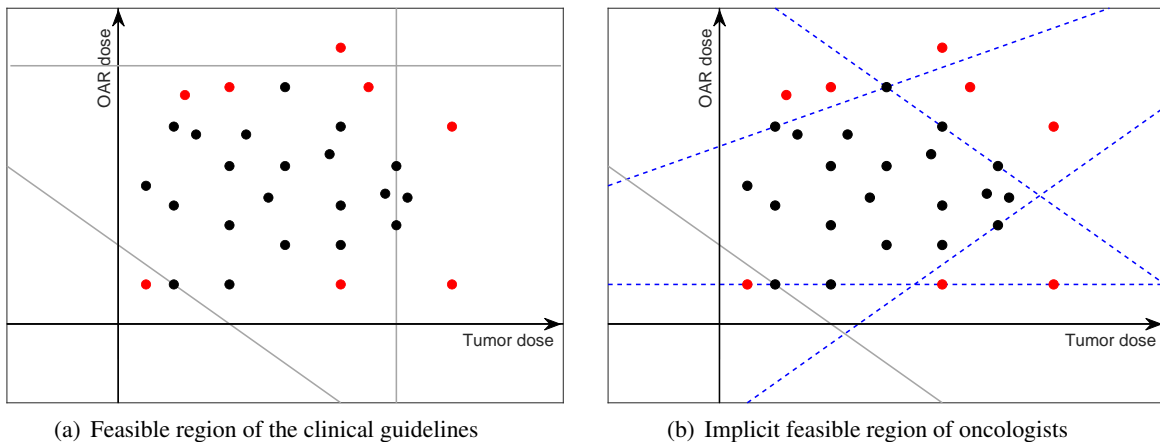


Figure 1 Simplified schematic representation of convex feasible regions based on guidelines (gray solid) versus implicit (blue dashed) constraints of oncologists. The black and red dots denote accepted and rejected plans, respectively.

1.2. Contributions

This paper aims to recover the underlying convex feasible region of a forward problem based on both accepted and rejected observations of past decisions. The goal is to provide a streamlined process to replace the current ill-fitting optimization models that are used as guidelines in practice to find the optimal solutions to a forward problem, and hence, the resulting solutions undergo iterative revisions with practical expert-driven guidelines. Using historical expert opinions, the goal of the proposed IO methodology is to learn a structured optimization model that can later be used in a forward setting to generate decisions that mimic successful decisions that have been accepted by experts in the past. The optimal solutions of such a learned model will facilitate and streamline the approval process by avoiding historically unacceptable solutions. The specific contributions of this paper are as follows.

1. We propose an inverse model to recover a fully- or partially-unknown convex feasible region of a forward optimization problem.
2. The proposed inverse model inputs both accepted and rejected decisions that guide the shape of the imputed feasible region for the forward problem.
3. We propose a reformulation of the proposed model using variational inequalities to reduce its computational complexity.
4. We demonstrate an application of the proposed methodology in standardizing the radiotherapy clinical guidelines for cancer treatment.

In the remainder of this paper, we first define our forward optimization problem mathematically and present the proposed inverse optimization model in Section 2. Next, in Section 3, we present a reformulation of the proposed inverse model to mitigate its computational complexity. Finally, we apply our methods to an example of deriving clinical guidelines for radiation therapy treatment planning for breast cancer patients in Section 4, and conclude the paper in Section 7.

2. Methodology

In this section, we first formulate a forward optimization problem with convex constraints, where all or some of the constraints are unknown. We then define the inverse problem mathematically where a set of accepted and rejected observations are given, and the goal is to find constraint parameters that correctly classify these observations while enforcing optimality conditions on a preferred solution. We then present our expert-guided inverse optimization model and characterize the properties of its solutions.

2.1. Problem Definition

Let \mathcal{I} be the set of all constraints in a forward optimization problem. We denote the set of known nonlinear and linear constraints by \mathcal{N} and \mathcal{L} , respectively, and the set of unknown nonlinear and linear constraints

to be inferred by $\tilde{\mathcal{N}}$ and $\tilde{\mathcal{L}}$, respectively. Note that $\mathcal{N} \cup \mathcal{L} \cup \tilde{\mathcal{N}} \cup \tilde{\mathcal{L}} = \mathcal{I}$ and $\mathcal{N}, \mathcal{L}, \tilde{\mathcal{N}}, \tilde{\mathcal{L}}$ are mutually exclusive sets. We note that the known constraints are a trusted subset of the guidelines that need to be satisfied by all future solutions, which can potentially be an empty set. Assume that the decision variable is $\mathbf{x} \in \mathbb{R}^m$. Consider a rational decision maker with a differentiable monotone convex objective function $f(\mathbf{x}; \mathbf{c})$ and let $g_n(\mathbf{x}; \mathbf{q}_n), \forall n \in \mathcal{N}$ be differentiable concave functions on \mathbf{x} . The convex forward optimization (FO) model can be formulated as:

$$\text{FO:} \quad \underset{\mathbf{x}}{\text{minimize}} \quad f(\mathbf{x}; \mathbf{c}) \quad (1a)$$

$$\text{subject to} \quad g_n(\mathbf{x}; \mathbf{q}_n) \geq \mathbf{0}, \quad \forall n \in \mathcal{N} \cup \tilde{\mathcal{N}} \quad (1b)$$

$$\mathbf{a}'_\ell \mathbf{x} \geq b_\ell. \quad \forall \ell \in \mathcal{L} \cup \tilde{\mathcal{L}} \quad (1c)$$

Note that because $g_n(\mathbf{x}, \mathbf{q}_n)$ is concave, the nonlinear constraints (1b) and linear constraints (1c) form a convex feasible region. For brevity of notations, let the set of all known constraints be defined as $\mathcal{X} = \{\mathbf{x} \in \mathbb{R}^m \mid g_n(\mathbf{x}; \mathbf{q}_n) \geq \mathbf{0}, \forall n \in \mathcal{N}, \mathbf{a}'_\ell \mathbf{x} \geq b_\ell, \forall \ell \in \mathcal{L}\}$, the region identified by the known constraints of FO. Given that the objective function (1a) minimizes a convex monotone function $f(\mathbf{x}; \mathbf{c})$, the optimal solution of FO is always on the boundary of its feasible region.

Assume that the structures of the functions $g_n(\mathbf{x}; \mathbf{q}_n), \forall n \in \mathcal{N}$ are known, and the goal is to find unknown parameters $\mathbf{q}_n, \forall n \in \tilde{\mathcal{N}}$. Note $\mathbf{a}_\ell \in \mathbb{R}^m$ and $b_\ell \in \mathbb{R}$ are parameters of fixed size while each \mathbf{q}_n might be a vector of a different length $\mathbf{q}_n \in \mathbb{R}^{\phi_n}$, where ϕ_n depends on the type of nonlinear function that is to be inferred. For example, $g_1(\mathbf{x}; \mathbf{q}_1) = q_{11}x_1^2 + q_{12}x_2^2 + q_{13}x_1x_2 + q_{14}$ is a two-dimensional quadratic function with four unknown parameters q_{11}, \dots, q_{14} to be inferred. In what follows, we describe the proposed inverse methodology for imputing the constraint parameters of the FO model.

2.2. Inverse Problem Formulation

Let $\mathbf{x}^k, k \in \mathcal{K}$ denote a set of given solutions corresponding to past decisions, where $\mathcal{K} = \mathcal{K}^+ \cup \mathcal{K}^-$ and \mathcal{K}^+ and \mathcal{K}^- denote accepted and rejected observed decisions, respectively. The goal of the inverse problem is to find a set of parameters $\mathbf{q}_n, \mathbf{a}_\ell$, and b_ℓ such that solving the corresponding FO model will result in an optimal solution that mimics the accepted observation and avoids the rejected ones. To this end, the inverse optimization problem infers a convex feasible region that would render all the past observations $\mathbf{x}^k, k \in \mathcal{K}^+$ as feasible for FO, and contrarily, all $\mathbf{x}^k, k \in \mathcal{K}^-$ as infeasible for FO.

Let \mathcal{H} be the convex hull of all accepted observations $\mathbf{x}^k, k \in \mathcal{K}^+$. We assume that the decision maker is rational and is solving an implicit convex optimization problem, which results in the observed data being well-posed and the inverse problem being feasible, as shown in Assumption 1.

ASSUMPTION 1. *The sets of given observations are well-posed and the forward problem is convex, i.e.,*

$$(a) \quad \exists \hat{\mathbf{q}}_n \in \mathbb{R}^{\phi_n}, \text{ such that } g_n(\mathbf{x}^k; \hat{\mathbf{q}}_n) \geq \mathbf{0}, \quad \forall n \in \tilde{\mathcal{N}}, k \in \mathcal{K}^+,$$

$$(b) \quad \mathbf{x}^k \in \mathcal{X}, \quad \forall k \in \mathcal{K}^+,$$

$$(c) \quad \nexists k \in \mathcal{K}^- \text{ such that } \mathbf{x}^k \in \mathcal{H}.$$

Assumption 1 ensures that the data and model are well-defined and that it is possible to construct a convex feasible region for FO. It states that (a) there exists a convex set that encapsulates the accepted observations, (b) the known constraints can indeed make the accepted observations feasible, and (c) the given input data do not contradict each other. These assumptions are not limiting given that the decision-maker is rational and is solving an implicit convex optimization problem. Note that if the data is not well-posed, a data pre-processing step and/or a notion of noise or error can be introduced in the inverse model. We further elaborate on such additions in Section 6.

Because the objective function $f(\mathbf{x}; \mathbf{c})$ is known in FO, we can identify the points in the convex hull of all accepted observations that provide the best objective value in FO. Definition 1 characterizes such a point as the ‘‘preferred solution’’. An example of the preferred solution for a convex objective function is visualized in Figure 2, where the blue dashed lines indicate iso-cost lines of the objective function and \mathbf{x}^0 is the preferred solution. This concept is formally introduced in Definition 1.

DEFINITION 1. The *preferred* solution $\mathbf{x}^0 \in \mathbb{R}^m$ is defined as

$$\mathbf{x}^0 \in \arg \min_{\mathbf{x} \in \mathcal{H}} \{f(\mathbf{x}; \mathbf{c})\}.$$

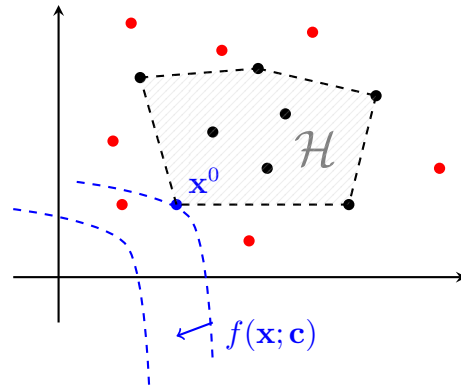


Figure 2 The preferred solution \mathbf{x}^0 has the best objective value among the convex hull of accepted observations.

Note that depending on the type of objective function and the shape of the convex hull \mathcal{H} , there may be multiple observations that satisfy the definition of a preferred solution, in which case, we arbitrarily label one of them as \mathbf{x}^0 . The preferred solution is not necessarily one of the observations, but it is always on the boundary of the convex hull of all observations.

The goal of this paper is to compute a set of linear and nonlinear constraints for the FO problem such that the accepted/rejected observations are inside/outside the inferred feasible region, respectively, and a preferred solution is an optimal solution for the FO model with the inferred feasible set. Hence, the intersection of the known constraints and the inferred constraints must include all the accepted observations and none of the rejected ones, providing a separation between the accepted and rejected points. We will refer to such a set of inferred constraints as a “nominal set”, as formally defined in Definition 2.

DEFINITION 2. A convex set $\tilde{\mathcal{X}}$ is a *nominal set* if

$$\begin{aligned} \mathbf{x}^k &\in \tilde{\mathcal{X}} \cap \mathcal{X} & \forall k \in \mathcal{K}^+, \\ \mathbf{x}^k &\notin \tilde{\mathcal{X}} \cap \mathcal{X} & \forall k \in \mathcal{K}^-. \end{aligned}$$

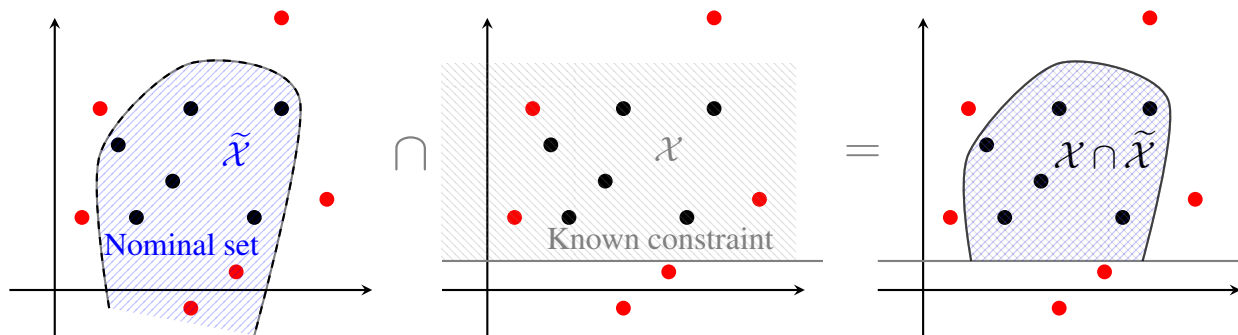


Figure 3 An illustration of the intersection of a nominal set and known constraints.

A simplified two-dimensional schematic of a nominal set is depicted in Figure 3. We note that different sets of constraints can result in the same nominal set geometrically. Hence, the goal of the inverse problem

is to find constraint parameters $\mathbf{a}_\ell, b_\ell, \forall \ell \in \tilde{\mathcal{L}}$, and $\mathbf{q}_n, \forall n \in \tilde{\mathcal{N}}$ such that the resulting inferred feasible set $\tilde{\mathcal{X}}$ is a nominal set, and the preferred solution \mathbf{x}^0 is an optimal solution for

$$\begin{aligned} & \underset{\mathbf{x}}{\text{minimize}} && f(\mathbf{x}; \mathbf{c}) \\ & \text{subject to} && \mathbf{x} \in \mathcal{X} \cap \tilde{\mathcal{X}}. \end{aligned}$$

To impute such constraints, we propose an expert-guided inverse optimization (GIO) formulation that imposes feasibility constraints on the accepted observations, ensures the infeasibility of the rejected points, and enforces optimality conditions on the preferred solution \mathbf{x}^0 . The GIO model can be written as follows.

$$\text{GIO: } \underset{\mathbf{a}, b, \mathbf{q}, \lambda, \mu, y}{\text{Maximize}} \quad \mathcal{D} \left(\mathbf{q}_1, \dots, \mathbf{q}_{|\tilde{\mathcal{N}}|}, \mathbf{A}, \mathbf{b}; (\mathbf{x}^1, \dots, \mathbf{x}^{|\mathcal{K}|}) \right) \quad (2a)$$

$$\text{subject to} \quad g_n(\mathbf{x}^k; \mathbf{q}_n) \geq \mathbf{0}, \quad \forall k \in \mathcal{K}^+, n \in \tilde{\mathcal{N}} \quad (2b)$$

$$\mathbf{a}'_\ell \mathbf{x}^k \geq b_\ell, \quad \forall k \in \mathcal{K}^+, \ell \in \tilde{\mathcal{L}} \quad (2c)$$

$$\nabla f(\mathbf{x}^0; \mathbf{c}) + \sum_{n \in \mathcal{N} \cup \tilde{\mathcal{N}}} \lambda_n \nabla g_n(\mathbf{x}^0, \mathbf{q}_n) + \sum_{\ell \in \mathcal{L} \cup \tilde{\mathcal{L}}} \mu_\ell \mathbf{a}_\ell = \mathbf{0}, \quad (2d)$$

$$\lambda_n g_n(\mathbf{x}^0, \mathbf{q}_n) = 0, \quad \forall n \in \mathcal{N} \cup \tilde{\mathcal{N}} \quad (2e)$$

$$\mu_\ell (b_\ell - \mathbf{a}'_\ell \mathbf{x}^0) = 0, \quad \forall \ell \in \mathcal{L} \cup \tilde{\mathcal{L}} \quad (2f)$$

$$\mathbf{a}'_\ell \mathbf{x}^k \leq b_\ell - \epsilon + M y_{\ell k}, \quad \forall \ell \in \mathcal{L} \cup \tilde{\mathcal{L}}, k \in \mathcal{K}^- \quad (2g)$$

$$g_n(\mathbf{x}^k; \mathbf{q}_n) \leq \mathbf{0} - \epsilon + M y_{nk}, \quad \forall n \in \mathcal{N} \cup \tilde{\mathcal{N}}, k \in \mathcal{K}^- \quad (2h)$$

$$\sum_{i \in \mathcal{I}} y_{ik} \leq |\mathcal{I}| - 1, \quad \forall k \in \mathcal{K}^- \quad (2i)$$

$$\mathbf{a}_\ell \in \mathcal{A}_\ell, b_\ell \in \mathcal{B}_\ell, \quad \forall \ell \in \tilde{\mathcal{L}} \quad (2j)$$

$$\mathbf{q}_n \in \mathcal{Q}_n, \quad \forall n \in \tilde{\mathcal{N}} \quad (2k)$$

$$\lambda_n, \mu_\ell \leq 0, \quad \forall n \in \mathcal{N} \cup \tilde{\mathcal{N}}, \ell \in \mathcal{L} \cup \tilde{\mathcal{L}} \quad (2l)$$

$$y_{ik} \in \{0, 1\}, \quad \forall i \in \mathcal{I}, k \in \mathcal{K}^-. \quad (2m)$$

The objective function (2a) maximizes a measure of distance between the constraint parameters and the observations. An example of the objective function can be maximizing the total distance between the inferred constraints and all the infeasible observations using a desirable distance matrix \mathcal{D} . We provide more details on this objective function example in Section 3.3. Constraints (2b) and (2c) enforce primal feasibility conditions. Constraints (2d) capture the stationarity conditions. Complementary slackness for the linear and nonlinear constraints of FO are captured in (2e) and (2f), respectively. Constraints (2g)–(2i) ensure that at least one constraint is violated by each of the rejected observations. Constraints (2j)–(2k) provide a set of desirable conditions on the coefficients of the imputed constraints such as normalization or convexity conditions. As an optional step, any other desirable condition on the parameters can also be included in \mathcal{Q} , and similar conditions on the linear constraint parameters can also be considered as $\mathbf{a}_\ell \in \mathcal{A}$, $b_\ell \in \mathcal{B}$. Lastly, constraints (2l)–(2m) indicate sign and binary declarations.

We next show that any optimal solution produced by the GIO model exhibits the desired properties of an inferred feasible region for FO.

PROPOSITION 1. *Any feasible solution of GIO corresponds to a nominal set $\tilde{\mathcal{X}}$ such that $\mathbf{x}^0 \in \arg \min_{\mathbf{x} \in \mathcal{X} \cap \tilde{\mathcal{X}}} \{f(\mathbf{x}; \mathbf{c})\}$.*

As Proposition 1 states, any solution of GIO has the properties of a nominal feasible set for FO and makes \mathbf{x}^0 optimal for the forward problem. To fulfill this requirement, GIO inserts at least one conflicting constraint per rejected observation such that the rejected observation becomes infeasible for FO while ensuring none of the accepted observations are cut off. Assuming that the forward model allows us to infer as many constraints as needed to do so, then it is always possible to find a solution for GIO.

PROPOSITION 2. For sufficiently large $|\tilde{\mathcal{L}}| + |\tilde{\mathcal{N}}|$, GIO is guaranteed to be feasible.

Proposition 2 states that GIO is feasible when the number of inferred constraints is sufficiently large. Next, in Remark 1, we construct an upper bound on the minimum number of constraints needed to make GIO feasible.

REMARK 1. An upper bound to the minimum number of required constraints in GIO is $|\mathcal{K}^-| + 1$. Depending on the number of rejected observations and their spatial distribution, a small number of constraints may be sufficient to cut off a large number of rejected observations. However, in the worst case, we would need one constraint per rejected observation to guarantee that each rejected point is infeasible for FO while ensuring the feasibility of all accepted points. We also need at least one inferred constraint ensuring that the preferred solution \mathbf{x}^0 is optimal for FO. We note again that one constraint may serve multiple purposes, which would result in a lower number of constraints needed in practical settings. For instance, a single constraint may cut a large number of rejected points out of the inferred feasible region.

The proposed GIO model (2) can be a very complex mixed-integer nonlinear problem which can pose a challenge for state-of-the-art commercial solvers. In Section 3, we propose a method for mitigating the complexity of the proposed inverse problem.

3. Mitigating Inverse Problem Complexity

The complexity of the GIO model (2) depends on the complexity of the FO model (1). Additionally, it includes KKT conditions of complementary slackness and stationarity, which can be nonlinear and non-convex. In the context of recovering linear constraint sets, prior work used linear programming duality to replace the optimality conditions and provide a tractable reformulation (Ghobadi and Mahmoudzadeh 2021).

To mitigate the complexity of inferring nonlinear constraints, we propose a tractable reformulation for solving GIO leveraging the concept of variational inequalities (Bertsimas et al. 2015b, Harker and Pang 1990, Kinderlehrer and Stampacchia 2000) to identify a linear constraint that can enforce optimality conditions instead of the nonlinear KKT conditions, generalizing the approach of Ghobadi and Mahmoudzadeh (2021) to nonlinear cases.

In what follows, we first introduce a few definitions and discuss preliminaries for constructing the reformulation. We then discuss the properties of an optimal inverse solution and provide problem-specific sufficient optimality conditions to replace the KKT criteria. Lastly, we present a reduced reformulation of the inverse problem.

3.1. Preliminaries and Definitions

Recall that the preferred solution \mathbf{x}^0 is optimal for FO and has a better objective value for $f(\mathbf{x}; \mathbf{c})$ than any other accepted observation. This characteristic relates to the well-studied concept of variational inequalities (Harker and Pang 1990), which we use to define a sublevel set in definition 3.

DEFINITION 3. The set \mathcal{V} is a *sublevel set* of $f(\mathbf{x}; \mathbf{c})$ at \mathbf{x}^0 defined as

$$\mathcal{V} = \{\mathbf{x} \in \mathbb{R}^n \mid f(\mathbf{x}; \mathbf{c}) \geq f(\mathbf{x}^0; \mathbf{c})\}.$$

Note that the sublevel set of the objective function at the preferred solution \mathbf{x}^0 contains all accepted observations because $f(\mathbf{x}^0; \mathbf{c}) \leq f(\mathbf{x}^k; \mathbf{c})$, $\forall k \in \mathcal{K}^+$. Solving minimize $f(\mathbf{x}; \mathbf{c})$ to optimality is equivalent to finding \mathbf{x}^0 that satisfies these variational inequality conditions. Since $f(\mathbf{x}; \mathbf{c})$ is convex and differentiable, we use its first-order condition to define a linear tangent to the sublevel set at \mathbf{x}^0 , as stated in Definition 4.

DEFINITION 4. The tangent half-space \mathcal{C} to the sublevel set of $f(\mathbf{x}; \mathbf{c})$ at \mathbf{x}^0 is defined as

$$\mathcal{C} = \{\mathbf{x} \in \mathbb{R}^n \mid (\nabla f(\mathbf{x}^0; \mathbf{c}))' \mathbf{x} \geq \nabla f(\mathbf{x}^0; \mathbf{c})' \mathbf{x}^0\}.$$

Simplified schematics of a sublevel set and its tangent half-space are shown in Figure 4. It can be seen that if $f(\mathbf{x}; \mathbf{c})$ is linear, the tangent half-space is equivalent to the sublevel set of $f(\mathbf{x}; \mathbf{c})$ at \mathbf{x}^0 , i.e., $\mathcal{C} = \mathcal{V}$. In the rest of this paper, we use \mathcal{C} to denote the tangent half-space of the sublevel set of $f(\mathbf{x}; \mathbf{c})$ at \mathbf{x}^0 , for brevity.

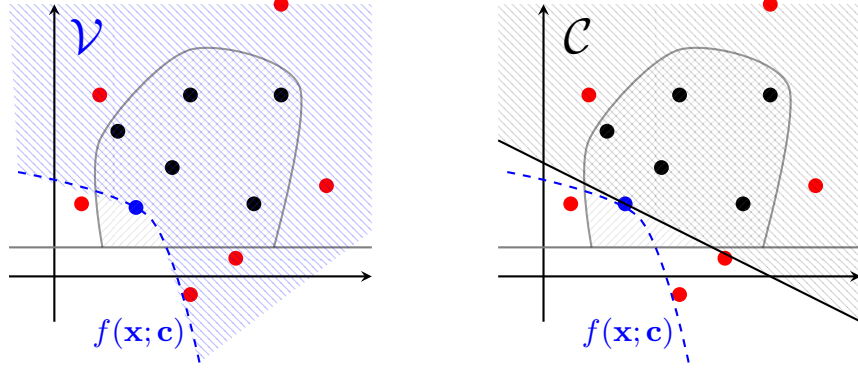


Figure 4 The sublevel set of $f(\mathbf{x}; \mathbf{c})$ (left) and its tangent half-space (right) at \mathbf{x}^0 .

3.2. Reduced Formulation

One of the key complexities of the GIO formulation is the inclusion of nonlinear KKT conditions for stationarity and complementary slackness, which ensure the optimality of the preferred solution. In this section, we leverage the concept of variational inequalities, which characterize solutions to inequalities over a feasible region, to find alternative formulation to the nonlinear KKT conditions. To this end, we use the half-space \mathcal{C} that is defined based on variational inequalities (see Definition 3). This half-space is tangent to sublevel sets of $f(\mathbf{x}; \mathbf{c})$ at \mathbf{x}^0 , and hence, enforces the optimality conditions of \mathbf{x}^0 , as detailed in Proposition 4. By replacing the KKT conditions with half-space \mathcal{C} , we arrive at a reduced formulation with less complexity than the original GIO model. For brevity of notations, we refer to any feasible region that is inferred using the GIO model as an *imputed set* for the forward problem. Given the properties of GIO solution outlined in Proposition 1, Definition 5 characterizes an imputed set for FO.

DEFINITION 5. Any convex nominal set $\mathcal{S} = \mathcal{X} \cap \tilde{\mathcal{X}}$ such that $\mathbf{x}^0 \in \arg \min_{\mathbf{x} \in \mathcal{X} \cap \tilde{\mathcal{X}}} \{f(\mathbf{x}; \mathbf{c})\}$ is an *imputed set* for FO.

We note that different GIO solutions may result in the same imputed set since it is a geometric representation of the feasible region, as opposed to an algebraic one. For instance, in a GIO solution, multiplying the coefficients of a linear constraint by a constant would result in a different solution, which may even be infeasible for GIO, but it would represent the same feasible set for FO. Proposition 3 shows that any imputed set as defined in Definition 5 is always contained within the tangent half-space \mathcal{C} .

PROPOSITION 3. If a $\mathcal{S} = \mathcal{X} \cap \tilde{\mathcal{X}}$ is an imputed set for FO then $\mathcal{S} \subseteq \mathcal{C}$.

Figure 5 shows the intuition behind Proposition 3 which states any imputed set for FO must be contained within the tangent half-space \mathcal{C} . Consider the convex nominal set \mathcal{S} denoted by the dashed green area, which is not contained within \mathcal{C} . Then \mathcal{S} must contain points outside of \mathcal{C} that are either in $\mathcal{V} \setminus \mathcal{C}$ or in the complement of \mathcal{V} . If \mathcal{S} contains $\hat{\mathbf{x}}' \notin \mathcal{V}$, then it cannot be an imputed set, by definition, since $\hat{\mathbf{x}}'$ dominates \mathbf{x}^0 and hence $\mathbf{x}^0 \notin \arg \min_{\mathbf{x} \in \mathcal{S}} \{f(\mathbf{x}; \mathbf{c})\}$. If \mathcal{S} contains a point $\hat{\mathbf{x}} \in \mathcal{V} \setminus \mathcal{C}$, then because $f(\mathbf{x}; \mathbf{c})$ is convex, there exists a convex combination of \mathbf{x}^0 and $\hat{\mathbf{x}}$ that dominates \mathbf{x}^0 and hence, again, $\mathbf{x}^0 \notin \arg \min_{\mathbf{x} \in \mathcal{S}} \{f(\mathbf{x}; \mathbf{c})\}$, which contradicts the definition of an imputed set. Proposition 3 provides a guideline for constructing an imputed set by intersecting any convex nominal set with the tangent half-space \mathcal{C} , as outlined in Proposition 4.

PROPOSITION 4. For any convex nominal set \mathcal{S} , the set $\mathcal{S} \cap \mathcal{C}$ is an imputed set.

Proposition 4 illustrates that the optimality condition on \mathbf{x}^0 can always be guaranteed if \mathcal{C} is used as one of the constraints in shaping the imputed set. Because any imputed set must be a subset of the tangent half-space \mathcal{C} , as shown in Proposition 3, the addition of \mathcal{C} does not exclude or cut any possible imputed sets for FO. Hence, instead of searching for a nominal set that satisfies the optimality on \mathbf{x}^0 , we can add the tangent half-space \mathcal{C} as one of the known constraints for FO, thereby, always guaranteeing that \mathbf{x}^0 will be the optimal solution of FO for any inferred feasible set. This additional constraint allows us to relax the

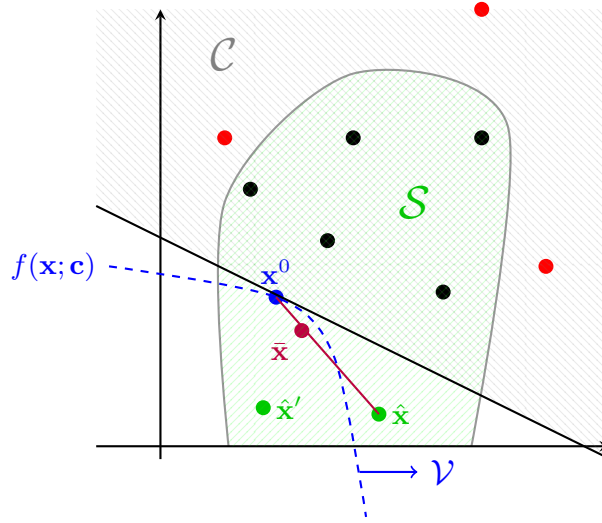


Figure 5 A convex nominal set $S \subseteq C$, to show the intuition behind the proof of Proposition 3

KKT conditions on the optimality of \mathbf{x}^0 in the GIO formulation and derive a reduced formulation, presented in Theorem 1.

THEOREM 1. *If C is appended to the known constraints of FO, solving GIO is equivalent to solving the following reduced model:*

$$\text{RGIO : } \underset{\mathbf{a}, \mathbf{b}, \mathbf{q}, \mathbf{y}}{\text{Maximize}} \quad \mathcal{D} \left(\mathbf{q}_1, \dots, \mathbf{q}_{|\tilde{\mathcal{N}}|}, \mathbf{A}, \mathbf{b}; (\mathbf{x}^1, \dots, \mathbf{x}^{|\mathcal{K}|}) \right) \quad (3a)$$

$$\text{subject to } g_n(\mathbf{x}^k; \mathbf{q}_n) \geq \mathbf{0}, \quad \forall k \in \mathcal{K}^+, n \in \tilde{\mathcal{N}} \quad (3b)$$

$$\mathbf{a}'_\ell \mathbf{x}^k \geq b_\ell, \quad \forall k \in \mathcal{K}^+, \ell \in \tilde{\mathcal{L}} \quad (3c)$$

$$\mathbf{a}_\ell \mathbf{x}^k \leq b_\ell - \epsilon + M y_{\ell k}, \quad \forall \ell \in \mathcal{L} \cup \tilde{\mathcal{L}}, k \in \mathcal{K}^- \quad (3d)$$

$$g_n(\mathbf{x}^k; \mathbf{q}_n) \leq \mathbf{0} - \epsilon + M y_{nk}, \quad \forall n \in \mathcal{N} \cup \tilde{\mathcal{N}}, k \in \mathcal{K}^- \quad (3e)$$

$$\sum_{i \in \mathcal{I}} y_{ik} \leq |\mathcal{I}| - 1, \quad \forall k \in \mathcal{K}^- \quad (3f)$$

$$\mathbf{a}_\ell \in \mathcal{A}_\ell, b_\ell \in \mathcal{B}_\ell, \quad \forall \ell \in \tilde{\mathcal{L}} \quad (3g)$$

$$\mathbf{q}_n \in \mathcal{Q}_n, \quad \forall n \in \tilde{\mathcal{N}} \quad (3h)$$

$$y_{ik} \in \{0, 1\}, \quad \forall i \in \mathcal{I}, k \in \mathcal{K}^-. \quad (3i)$$

We note that RGIO is always feasible because it is a relaxed version of GIO with fewer constraints, and we know from Proposition 2 that GIO is always feasible. Based on Theorem 1, to find an imputed set, we can simply find a nominal feasible set and super-impose the known constraints including the tangent halfspace of the sublevel set of $f(\mathbf{x}; \mathbf{c})$ at the preferred solution \mathbf{x}^0 .

COROLLARY 1. *RGIO infers unknown constraints $\tilde{\mathcal{X}}$ that shape a nominal feasible set for FO such that \mathbf{x}^0 is an optimal solution of*

$$\underset{\mathbf{x}}{\text{minimize}} \quad f(\mathbf{x}; \mathbf{c}) \quad (4a)$$

$$\text{subject to } \mathbf{x} \in C \cap \mathcal{X} \cap \tilde{\mathcal{X}}. \quad (4b)$$

Corollary 1 provides a method for reducing the complexity of the GIO model. In Section 3.4, we provide a numerical example that illustrates how an imputed set can be constructed using Corollary 1.

The RGIO model eliminates the need for explicitly writing the stationarity and complementary slackness constraints because the inclusion of the tangent half-space \mathcal{C} makes them redundant for the GIO model. Because \mathcal{C} is a tangent half-space of the sublevel set of $f(\mathbf{x}; \mathbf{c})$ at the preferred solution \mathbf{x}^0 , its inclusion ensures that the resulting inferred feasible region is an imputed set. The only constraints that are required to remain in the RGIO model are those that ensure the imputed constraints form a nominal solution that includes all accepted observations and none of the rejected ones. Therefore, the size of the RGIO problem is considerably lower than that of the GIO problem, and it relaxes a large number of nonconvex nonlinear constraints. A comparison of the number of variables and constraints in the GIO and RGIO models is provided in Table 1.

	Type	Model	Count
Variables	Continuous	GIO	$(m+2) \tilde{\mathcal{L}} + (\phi+1) \tilde{\mathcal{N}} + \mathcal{N} + \mathcal{L} $
		RGIO	$(m+1) \tilde{\mathcal{L}} + \phi \tilde{\mathcal{N}} $
	Binary	GIO	$(\mathcal{N} + \mathcal{L} + \tilde{\mathcal{N}} + \tilde{\mathcal{L}}) \mathcal{K}^- $
		RGIO	$(\mathcal{N} + \mathcal{L} + \tilde{\mathcal{N}} + \tilde{\mathcal{L}}) \mathcal{K}^- $
Constraints	Linear	GIO	$ \tilde{\mathcal{L}} (\mathcal{K}^+ + 1) + (\mathcal{L} + 1) \mathcal{K}^- $
		RGIO	$ \tilde{\mathcal{L}} (\mathcal{K}^+ + 1) + (\mathcal{L} + 1) \mathcal{K}^- $
	Nonlinear	GIO	$ \tilde{\mathcal{N}} (\mathcal{K}^+ + \mathcal{K}^- + 1) + \mathcal{N} (\mathcal{K}^- + 1) + m$
		RGIO	$ \tilde{\mathcal{N}} (\mathcal{K}^+ + \mathcal{K}^-) + \mathcal{N} \mathcal{K}^- $

Table 1 Comparison of the number of variables and constraints in the GIO and RGIO models.

Table 1 shows that the RGIO model has fewer continuous variables and nonlinear constraints compared to the GIO model. The nonlinear constraints that remain in RGIO primal feasibility constraints (i.e., $g_n(\mathbf{x}; \mathbf{q}) \geq 0$) which are nonlinear in \mathbf{x} , but may be linear (or be linearized) in \mathbf{q}_n , which is the decision variable in RGIO. Particularly, if the FO is linear, then the corresponding RGIO model can be linear integer if a linear distance metric is used in the objective function. In what follows, we discuss one example of a distance metric that can be used in the RGIO model.

3.3. Example of Distance Metric

The objective function in GIO and RGIO maximizes a non-negative distance metric between the inferred constraints and the observations. In this section, we provide an example of such a distance metric and write the complete GIO formulation based on it, which will be used in the application example presented in Section 4.

We consider an objective that aims to robustify against inclusion of rejected observations in the inferred feasible region by finding constraints that are as far as possible from the rejected observations and as close as possible to the accepted ones. To formulate this objective, we use Separation Distance, defined as maximizing the maximum distance between the inferred constraints to exclude each of the rejected observations, $\mathbf{x}^k, k \in \mathcal{K}^-$, from the inferred feasible set. That is, among the constraints that make each rejected observation infeasible, we select the constraint furthest away from the rejected observation and push it as close to the accepted observations as possible. Hence, we define the Separation Distance \mathcal{D} as

$$\mathcal{D}(\mathbf{q}_1, \dots, \mathbf{q}_{|\tilde{\mathcal{N}}|}, \mathbf{A}, \mathbf{b}; (\mathbf{x}^1, \dots, \mathbf{x}^{|\mathcal{K}^-|})) = \sum_{k \in \mathcal{K}^-} \max \left\{ \max_{\ell \in \tilde{\mathcal{L}}} \{d_{\ell k}([\mathbf{a}_\ell, b_\ell], \mathbf{x}^k)\}, \max \{d_{nk}(\mathbf{q}_n, \mathbf{x}^k)\} \right\},$$

where d_{ik} is the distance between the imputed constraint $i \in \tilde{\mathcal{L}} \cup \tilde{\mathcal{N}}$ and the rejected observation $k \in \mathcal{K}^-$. This objective can be linearized using a set of additional constraints as shown in model (5).

$$\text{Maximize}_{\mathbf{a}, b, \mathbf{p}, y, z} \sum_{k \in \mathcal{K}^-} z_k \quad (5a)$$

$$\text{subject to } d_{nk} \geq -g_n(\mathbf{x}^k; \mathbf{q}_n), \quad \forall n \in \tilde{\mathcal{N}}, k \in \mathcal{K}^- \quad (5b)$$

$$d_{nk} \leq -g_n(\mathbf{x}^k; \mathbf{q}_n) + My_{nk}, \quad \forall n \in \tilde{\mathcal{N}}, k \in \mathcal{K}^- \quad (5c)$$

$$d_{\ell k} \geq b_\ell - \mathbf{a}'_\ell \mathbf{x}^k, \quad \forall \ell \in \tilde{\mathcal{L}}, k \in \mathcal{K}^- \quad (5d)$$

$$d_{\ell k} \leq b_\ell - \mathbf{a}'_\ell \mathbf{x}^k + My_{\ell k}, \quad \forall \ell \in \tilde{\mathcal{L}}, k \in \mathcal{K}^- \quad (5e)$$

$$d_{ik} \leq M(1 - y_{ik}), \quad \forall i \in \tilde{\mathcal{N}} \cup \tilde{\mathcal{L}}, k \in \mathcal{K}^- \quad (5f)$$

$$d_{ik} \geq \epsilon(1 - y_{ik}), \quad \forall i \in \tilde{\mathcal{N}} \cup \tilde{\mathcal{L}}, k \in \mathcal{K}^- \quad (5g)$$

$$z_k \leq d_{ik} + Mp_{ik}, \quad \forall i \in \tilde{\mathcal{N}} \cup \tilde{\mathcal{L}}, k \in \mathcal{K}^- \quad (5h)$$

$$\sum_{i \in \mathcal{I}} p_{ik} \leq |\mathcal{I}| - 1, \quad \forall k \in \mathcal{K}^- \quad (5i)$$

$$p_{ik} \geq y_{ik}, \quad \forall i \in \tilde{\mathcal{N}} \cup \tilde{\mathcal{L}}, k \in \mathcal{K}^- \quad (5j)$$

$$(3b) - (3i). \quad (5k)$$

Constraints (5b)–(5g) find the slack distance between each rejected point and each constraint. Constraints (5h)–(5j) find the maximum distance of each constraint that makes each point infeasible, and the objective (5a) maximizes this maximum distance. The original primal feasibility constraints of the RGIO model are also enforced. Note that this specific distance model only requires the addition of linear constraints and binary variables, so if the FO is a linear problem, the corresponding RGIO problem will be a linear integer problem. Any other metric of interest can also be used in the objective, but for simplicity, we will use this linear metric in the application example in Section 4.

3.4. Illustrating Numerical Example

In this section, we provide an illustrative two-dimensional FO problem and formulate the corresponding RGIO formulation. We formulate a nonlinear FO model and its corresponding nonlinear mixed-integer RGIO model in AMPL Version: 3.1.1 and solve them both using Gurobi 11.0.3. All results are rounded to one decimal place.

EXAMPLE 1. Consider the following nonlinear convex FO problem

$$\text{minimize}_{\mathbf{x}} 2^{x_1} + x_2 \quad (6a)$$

$$\text{subject to } \frac{(x_1 - q_1)^2}{4} + \frac{(x_2 - q_2)^2}{2} \leq q_3, \quad (6b)$$

$$a_1 x_1 + a_2 x_2 \geq b, \quad (6c)$$

$$x_1, x_2 \geq 0. \quad (6d)$$

where x_1, x_2 are the decision variables, a_1, a_2 , and b are unknown parameters of the linear constraint (6c), and q_1, q_2 , and q_3 are the unknown parameters of the nonlinear convex constraint (6b). The non-negativity constraints (6d) are the only known constraints.

Let $\mathcal{K}^+ = \{1, \dots, 13\}$ and $\mathcal{K}^- = \{14, \dots, 21\}$ indicate 21 total observations, with 13 accepted observations $(\mathbf{x}^1, \dots, \mathbf{x}^{13}) = \begin{pmatrix} 1.5 & 2 & 2.5 & 3 & 4 & 4 & 1.5 & 3 & 3 & 3 & 4.8 & 2 & 5 \\ 1.5 & 2 & 1 & 3 & 2 & 3 & 2.5 & 1.5 & 3.4 & 2.5 & 2.4 & 3 & 2 \end{pmatrix}$ and 7 rejected observations $(\mathbf{x}^{14} \dots \mathbf{x}^{21}) = \begin{pmatrix} 4 & 4 & 1 & 3 & 1 & 1.5 & 5 \\ 1 & 3.5 & 3 & 4 & 1 & 3.5 & 1 \end{pmatrix}$. The preferred observation is $\mathbf{x}^0 = \begin{pmatrix} 1.5 \\ 1.5 \end{pmatrix}$ which leads to the \mathbf{x}^0 -sublevel set of $\mathcal{V} =$

$\{(x_1, x_2) \mid 2^{x_1} + x_2 \geq 2^{1.5} + 1.5\}$. Since the objective function (6a) is monotone, convex, and differentiable in x_1, x_2 , we can write the tangent half-space as

$$\begin{aligned} \mathcal{C} &= \{\mathbf{x} \in \mathbb{R}^n \mid (\nabla f(\mathbf{x}^0; \mathbf{c}))' \mathbf{x} \geq \nabla f(\mathbf{x}^0; \mathbf{c})' \mathbf{x}^0\} \\ \Rightarrow \mathcal{C} &= \begin{pmatrix} 2^{1.5} \ln 2 \\ 1 \end{pmatrix}' \begin{pmatrix} x_1 \\ x_2 \end{pmatrix} \geq \begin{pmatrix} 2^{1.5} \ln 2 \\ 1 \end{pmatrix}' \begin{pmatrix} 1.5 \\ 1.5 \end{pmatrix} \\ \Rightarrow \mathcal{C} &= (2^{1.5} \ln 2)x_1 + x_2 \geq (2^{1.5} \ln 2)(1.5) + 1.5. \end{aligned}$$

Considering this \mathcal{C} as a known constraint in FO, the RGIO model can be written as

$$\text{Maximize}_{\mathbf{a}, b, \mathbf{q}, \mathbf{y}} \mathcal{D}(q_1, \dots, q_3, \mathbf{a}, b; (\mathbf{x}^1, \dots, \mathbf{x}^{|\mathcal{K}|})) \quad (7a)$$

$$\text{subject to } q_3 - \frac{(x_1^k - q_1)^2}{4} - \frac{(x_2^k - q_2)^2}{2} \geq 0, \quad \forall k \in \mathcal{K}^+ \quad (7b)$$

$$q_3 - \frac{(x_1^k - q_1)^2}{4} - \frac{(x_2^k - q_2)^2}{2} \leq 0 - \epsilon + M y_{1k}, \quad \forall k \in \mathcal{K}^- \quad (7c)$$

$$\mathbf{a}' \mathbf{x}^k \geq b, \quad \forall k \in \mathcal{K}^+ \quad (7d)$$

$$\mathbf{a}' \mathbf{x}^k \leq b - \epsilon + M y_{2k}, \quad \forall k \in \mathcal{K}^- \quad (7e)$$

$$y_{1k} + y_{2k} \leq 1, \quad \forall k \in \mathcal{K}^- \quad (7f)$$

$$y_{1k}, y_{2k} \in \{0, 1\}, \quad \forall k \in \mathcal{K}^-. \quad (7g)$$

$$\text{other existing constraints.} \quad (7h)$$

Solving Formulation (7) using the Separation Distance metric \mathcal{D} as defined in Section 3.3 yields the optimal RGIO solution $(q_1, q_2, q_3) = (3.0, 2.0, 1.0)$ and $(a_1, a_2) = (-1, 2), b = -1$.

Figure 6 illustrates the input and output of the inverse model graphically. The feasible and infeasible observations are depicted as black and red dots, respectively. The inferred nonlinear and linear constraints are shown in the green ellipse and green linear half-space, respectively. The linear constraint makes the rejected point $(4, 1)$ infeasible, and the inferred ellipse makes the rest of the rejected observations (red) infeasible. The tangent half-space, shown as a solid black line marked by \mathcal{C} , which is considered a known constraint, enables the preferred solution, \mathbf{x}^0 to be optimal. The sublevel set of the objective function at \mathbf{x}^0 is shown in a solid blue curve and two other sample isocost curves are illustrated in dashed blue curves.

It can be seen that the intersection of the inferred or known constraints, i.e., $\mathcal{X} \cap \tilde{\mathcal{X}}$, only includes all accepted observations and excludes all the rejected observations. However, it does not have the preferred solution \mathbf{x}^0 on its boundary, and as a result, would not allow \mathbf{x}^0 to be optimal for FO. On the contrary, the tangent half-space \mathcal{C} allows for \mathbf{x}^0 to be a candidate optimal solution for FO when added as a known constraint. Hence, $\tilde{\mathcal{X}} \cap \mathcal{X} \cap \mathcal{C}$ is an imputed set for FO as it satisfies the properties outlined in Definition 5, which in this example is constructed using Corollary 1. \triangle

4. Application: Standardizing Clinical Radiation Therapy Guidelines

In this section, we test the proposed methodology using an application example on standardizing radiation therapy treatment planning guidelines for breast cancer patients. We first introduce the problem in the context of radiation therapy. Next, we describe the data and the experimental setup. Lastly, we present and discuss the results and provide practical insights.

4.1. Problem Description: Standardizing Clinical Radiation Therapy Guidelines

Breast cancer is the most widely diagnosed type of cancer in women worldwide. The cancerous tumor is often removed, leaving behind a cavity, and radiation treatment is subsequently prescribed to eliminate any remaining cancer cells. Tangential intensity-modulated radiation therapy (IMRT) is a treatment modality often used as part of the treatment for most breast cancer patients. In tangential IMRT, two opposing beams that are tangent to the external body of the patient are used to deliver radiation to the breast tissue. The

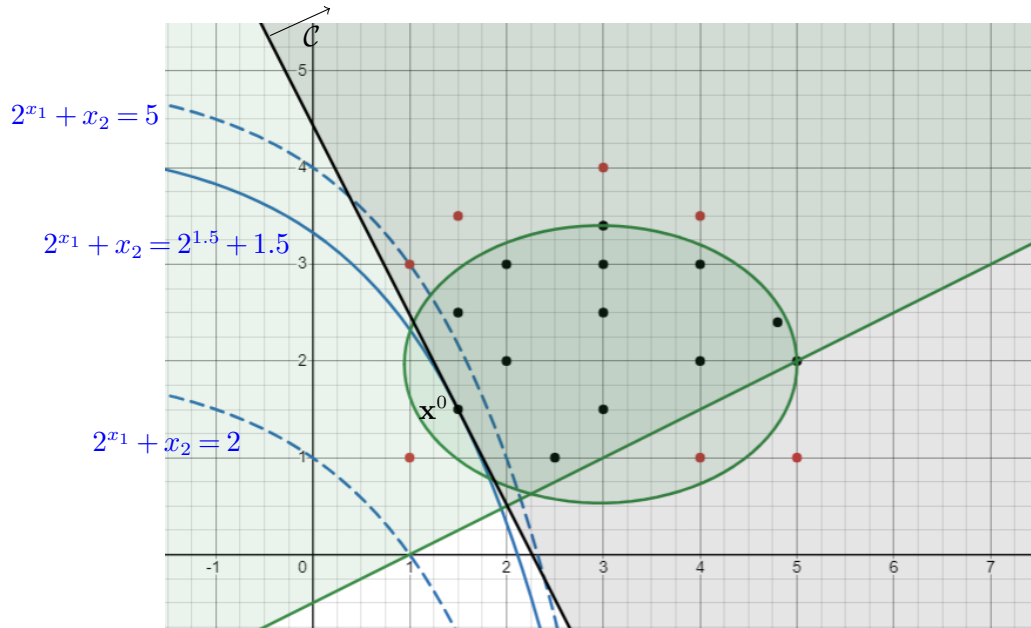


Figure 6 Numerical example for inferring a linear and a nonlinear constraint

main organ at risk in breast cancer IMRT is the heart, particularly when the left breast is being irradiated (Mahmoudzadeh et al. 2015). The goal is to find the radiation beam configurations from each angle such that the clinical target volume (CTV) inside the breast is fully irradiated and the heart is spared from radiation as much as possible. Figure 7 shows a computed tomography (CT) scan of a breast cancer patient along with the two tangential beams and the contours showing the organs at risk.

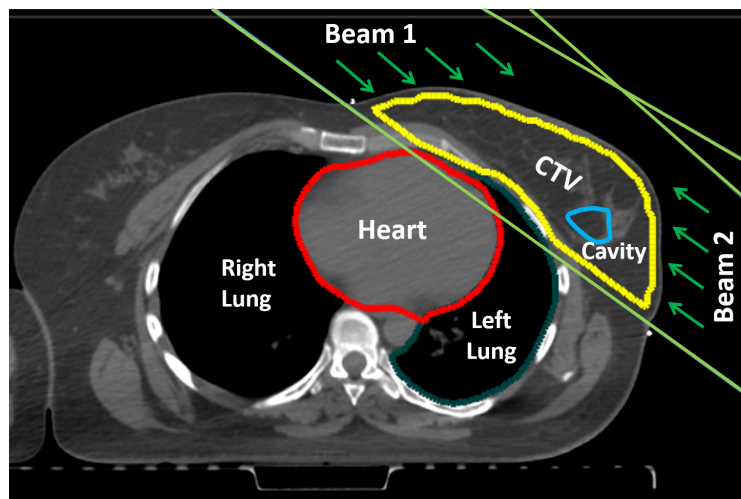


Figure 7 Computed Tomography (CT) scan of a breast cancer patient with important organs delineated. Image adapted from Mahmoudzadeh et al. (2015).

There is a set of acceptability guidelines in breast cancer treatment planning, which involve clinical dose-volume criteria on the CTV and the heart. A dose-volume criterion is a clinical metric that calculates the dose threshold to a certain fraction of an organ measured in units of radiation dose, Gray (Gy). For instance, the prescribed dose for the CTV is 42.4 Gy and at least 99% of the CTV must receive lower than 95% of the prescribed dose for a plan to be accepted. That is, if the body is discretized into three-dimensional cubes called voxels, then the 95% quantile of the voxels must receive a dose of $42.4 \times 0.95 = 40.28$ Gy or higher.

Similarly, at most 0.5% of the CTV can receive a dose higher than 108% of the prescribed dose, which means the dose to upper 0.5% quantile of the CTV must be lower than $1.08 \times 42.4 = 45.792$. There are also upper bounds on the dose delivered to the heart, where the highest-dosed 10 cc and 25 cc volume of the heart must receive a dose lower than 90% and 50% of the prescribed dose, respectively.

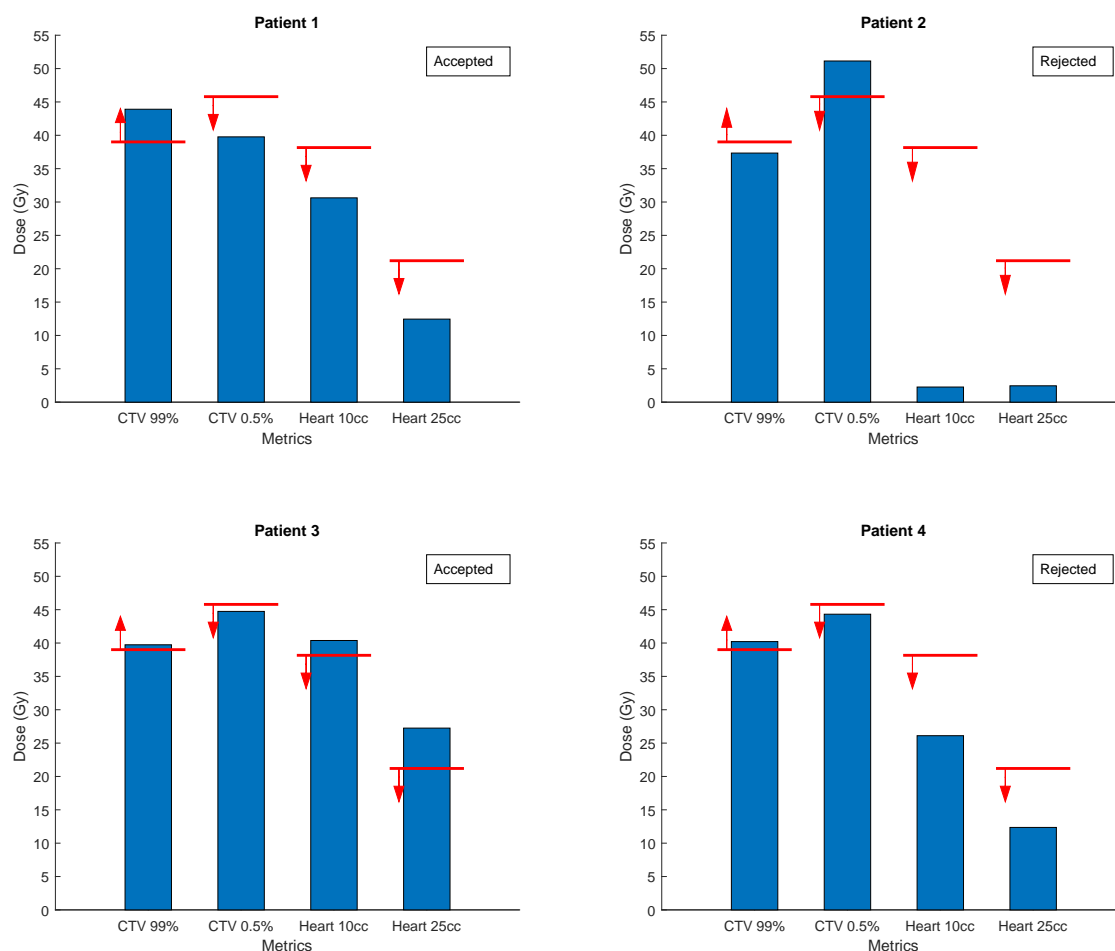


Figure 8 Hypothetical examples of accepted/rejected treatment plans. The guidelines are indicated with (red) lines on the bars and arrows indicate the direction of bounds.

These clinical dose-volume guidelines are used as a base reference for planning, but acceptance or rejection of the plan is at the discretion of oncologists. Figure 8 shows an example of possible clinical guidelines and metric values for four hypothetical patients that are labeled as accepted or rejected. It can be seen that the plan for Patient 1 and Patient 3 are accepted, while the plan for Patient 1 meets the guidelines but the plan for Patient 3 violates two of the dose-volume metrics on the heart. On the contrary, the plan for Patient 2 is rejected because it does not meet the guidelines, but the plan for Patient 4 is also rejected even though it meets all the guidelines. These inconsistencies typically stem from discrepancies between current clinical guidelines— which often are not data-driven, tailored to patient populations, or updated regularly — and the practical criteria that oncologists use in their day-to-day decisions to accept or reject treatment plans. This ambiguity in true underlying criteria can lead to unnecessary back-and-forth between oncologists and planners to arrive at an acceptable plan. In what follows, we provide more details about the patient data and existing clinical guidelines in Section 4.2, and discuss the details of the corresponding FO and IO models for this problem in Section 4.3.

Dose Metric	Clinical Limit	% met in past accepted plans data
Cavity1 min	≥ 40.28 Gy	50%
Cavity2 min	≥ 40.28 Gy	30%
CTV 99% min	≥ 39.01 Gy	39%
Heart 10cc max	≤ 38.16 Gy	100%
Lung 45 cc max	≤ 38.16 Gy	38%
CTV 0.5% max	≤ 45.79 Gy	57%
Heart 25 cc max	≤ 21.20 Gy	100%
Lung 25 cc max	≤ 36.04 Gy	40%

Table 2 The percentage of accepted plans that meet each of the criteria in the current guidelines.

4.2. Patient Data and Clinical Guidelines

We used retrospective clinical treatment plans for five breast cancer datasets to bootstrap and simulate a population of an additional 100 plans, to a total of 105 patients. We perturbed the structure-based radiation dose of each patient by 20% in a uniformly random manner to create an additional 20 synthetic patients per original patient. The prescribed dose for all patients, synthetic or original, is 42.4 Gy. Among the five original plans, four were deemed clinically acceptable, and one was rejected (with the patient ultimately receiving an alternate mode of treatment under breath-hold (Wong et al. 1999)). We assigned the same acceptable or rejected labels to the synthetic plans as the original plans that they are based on.

To inform the clinical treatment planning process, the plan for each of the patients is clinically measured through eight dose metrics, including maximum and minimum doses to different regions and dose-volume values for the CTV, the cavity, the heart, and the lung. These eight clinical guidelines and the accepted clinical limits are outlined in Table 2. The last column illustrates the percentage of accepted plans that met each of the clinical criteria, which confirms that there is wide variability in how rigorously the guidelines are imposed on accepted plans. For instance, while the Heart max dose guidelines are met by all accepted plans, the rest of the guidelines are only met by 30-60% of the plans. Similarly, 50% of all accepted patients met the clinical guideline of having at least 40.28 Gy dose to one of the cavity structures, highlighting that the clinical guidelines are not strictly followed in practice. We note that this dataset did not include any plans that met all the criteria but were rejected based on the current guidelines, perhaps an indication that these particular guidelines are collectively too tight. Similarly, there were no accepted plans that met all guideline criteria. In our analyses in Section 5, we use the criteria listed in Table 2 as clinical guidelines.

In addition to the features used in these clinical guidelines, we consider six other features in our models that may carry implicit clinical importance in final treatment plans, bringing the total to 14 clinical features. A summary of these features and their values for accepted and rejected patients is provided in Figure 9 where the error bars show the range of each metric for all patients in that category. As the figure illustrates, there is no clear separation between accepted and rejected plans and the underlying logic behind the acceptance/rejection decision cannot be inferred by just considering these metrics. Specific patient examples from this dataset were also previously shown in Figure 8.

4.3. Forward and Inverse Problem Description

We consider a forward optimization problem that imposes a set of clinical dosimetric criteria on the radiotherapy treatment plan for each patient. The objective of the forward problem is minimizing the maximum dose to the healthy tissue, and there is a set of known clinical criteria and unknown implicit constraints that affect the acceptability of a plan, as described in model (9) in Appendix B. The inverse model then inputs a set of past patient treatments which are labeled as accepted or rejected and infers a set of constraints that capture the underlying implicit constraints.

The inverse problem learns a set of implicit constraints to characterize the underlying feasible region of the oncologists' forward problem based on their historical accept/reject decisions. To do so, we employ the data described in Section 4.2 to infer 10 constraints using model (5) with the Separation Metric to maximize the distance between the inferred feasible region and the infeasible observations. For this application,

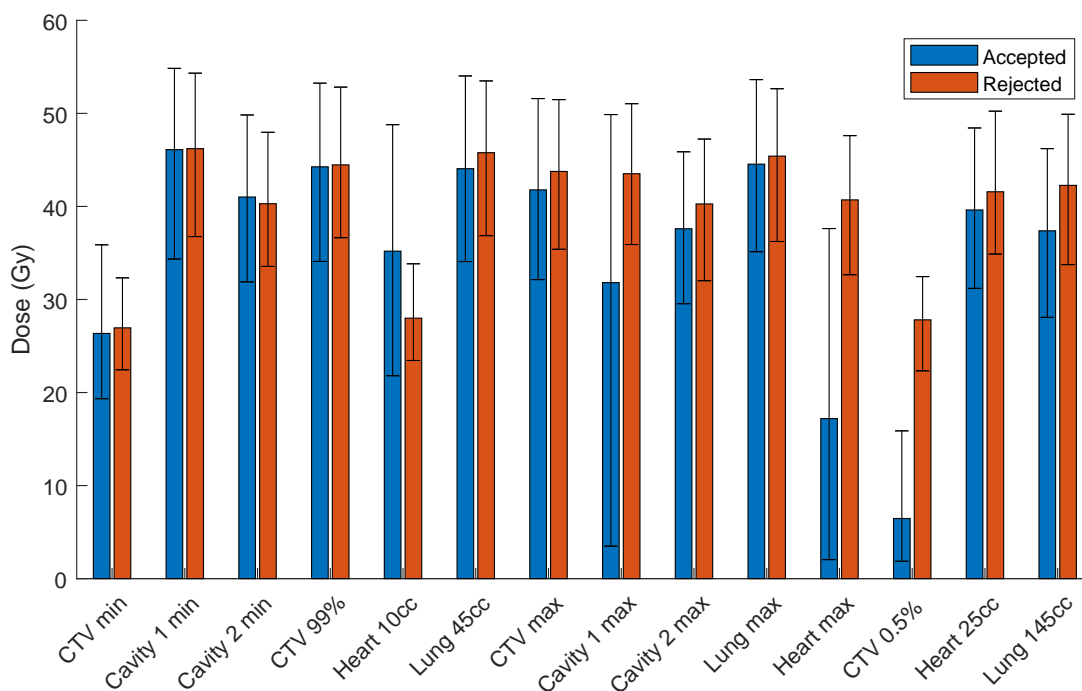


Figure 9 Visualization of a set of metrics calculated for all accepted and rejected plans. The errorbars show the range of each calculated metric across all plans in each category.

we considered linear constraints for the FO problem, which is relevant in practical settings for radiation therapy because clinical dose-volume criteria for breast cancer can be written as linear constraints using Conditional-Value-at-risk (CVaR) metrics (Chan et al. 2014a). The details of the RGIO model and the parameters used in this application are provided in Appendix B. We use these models to obtain results in Section 5.

5. Results

We use a random 60% of data detailed in Section 4.2, a mix of accepted and rejected plans, as input to the inverse model (10) to infer the proposed feasible region. We consider the remaining 40% of the data as future patients to test the IO methodology and validate the agreement of the inferred RGIO feasible region with the historical accept/reject decision of clinicians. To benchmark our inferred feasible region against the existing guidelines, we also test these guidelines against the entire dataset of accepted and rejected plans. The goal is to test whether using the inferred RGIO constraints and the clinical guidelines would render the accepted and rejected observations as feasible and infeasible for FO, respectively. Vice-versa, we also test whether the accepted and rejected plans align with the inferred constraints or the clinical guidelines. Tables 3 and 4 summarize these results.

Future patient plans	% Accepted ($\mu \pm \sigma$)	% Rejected ($\mu \pm \sigma$)
If plan is feasible for guidelines	N/A*	N/A*
If plan is feasible for RGIO	98.4 ± 0.03	1.6 ± 0.03

Table 3 Comparison of quality of RGIO vs guideline constraints when a plan meets all constraints.

*None of the future patient plans meet all the guidelines.

First, in Table 3, we separately consider plans that are rendered feasible/infeasible by the guidelines and then by the inferred RGIO constraints. The two columns show the percentage of the feasible/infeasible

plans according to each method that was historically accepted/rejected by clinicians, respectively. Upon observing the data, we noticed that none of the plans in our future patient dataset met all the guidelines, hence, we cannot calculate the required metric on an empty set. For the inferred RGIO constraints, on the contrary, an average of 98% of the plans that were feasible according to the inferred constraints were also accepted by the clinicians, with a small standard deviation of 0.03%.

Next, in Table 4, we perform the opposite analysis. Consider all the future patient plans that are accepted or rejected by clinicians. Table 4 shows the percentage of accepted plans that are also feasible with respect to the clinical guidelines and the inferred RGIO constraints. In line with what we observed in Table 3, none of the accepted plans were deemed feasible by the guidelines, while an average of 94.2% of the accepted plans were also deemed feasible by the inferred RGIO constraints.

Future patient plans	% Feasible for guidelines	% Feasible for RDIO
Accepted	0 % *	(94.2 ± 0.14)%
Rejected	100 % *	(5.8 ± 0.14) %

Table 4 Comparison of quality of RGIO vs. guideline constraints when a plan is infeasible.

*All future patient plans were infeasible according to guidelines.

The insights highlighted by Tables 3 and 4 confirm that using the clinical guidelines to generate plans is not helpful in practice because guidelines are too restrictive and impossible to meet in this dataset, whereas plans that are made based on RGIO inferred constraints are highly likely to be accepted by clinicians. Similarly, almost all clinically accepted plans meet all the RGIO inferred constraints, which is an indication that learning the acceptability criteria through RGIO can help in building plans that are acceptable to clinicians.

To further test the accuracy of the proposed inverse methodology, we calculated a set of standard metrics for out-of-sample prediction, including accuracy (% correct prediction), precision (% correct acceptable prediction), specificity (% correct rejection identification), recall (% correct acceptable identification), F1 Score (harmonic average of recall and precision). We tested the model using a similar 60/40 random split for past/future patients, repeated the split 50 times, ran the result for each split, and computed the average and the range for each metric. Figure 10 shows that the inverse model consistently performs well with an average performance between 95%–100% across all metrics. The lowest metric was specificity at 95%, which we believe is due to a low number of rejected observations in our dataset.

We next tested the sensitivity of the proposed method to the required number of past patients used to train the RGIO model. Figure 11 illustrates the trends of each metric when the number of past patients is varied between 20% to 80% of all patients in increments of 10%, with 250 random splits for each percentage. The x-axis shows the % of the data that was used as past patients (the rest used as future patients), and the y-axis shows how each metric performed (on average). The results show that the method works well across the board, even when using only 20% of the available data as past patients. We see a slight dip right before the 50-50 split but it picks up again when we pass the ratio. While there is always randomness, the methods seem to consistently obtain good results on average (with all metrics above 95%) at a 60-40 split. Even in the worst case, our recall and F1 scores are above 90%.

6. Limitations and Future Work

In this section, we review a few limitations of the presented work in this paper and provide directions for future research to address these limitations. We first discuss the need for data pre-processing (Section 6.1), followed by methods for handling ill-posed data and allowing misclassification (Section 6.2). We then discuss possible routes for mitigating data uncertainty (Section 6.3) and overfitting (Section 6.4), and finally highlight the key differences between the proposed approach with well-known classification approaches and motivate further benchmarking (Section 6.5).

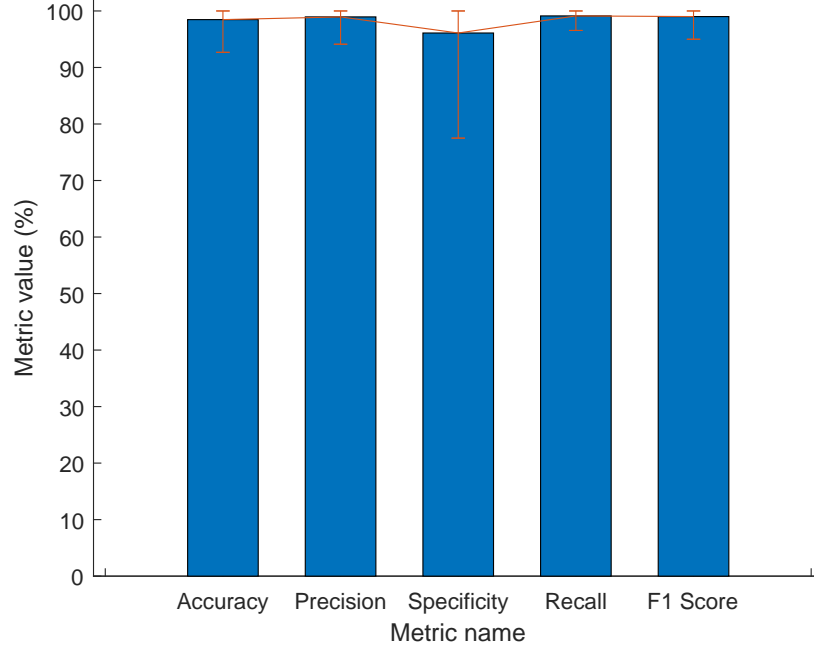


Figure 10 Out-of-sample performance of the inverse model using a 60/40 split for past/future patients.

6.1. Data Preprocessing

In our framework, data quality and pre-processing can play an important role in the size of our models and the quality of the obtained solutions. Simple pre-processing methods can potentially reduce the size of the observations by identifying and removing those observations that are already rendered infeasible by the known constraints. A reduction in the number of these infeasible observations can largely improve the complexity and size of the inverse problem. Any redundant observations or outliers can be removed from the set of observations using a data-cleaning method of choice.

Data pre-processing can also assist in ensuring acceptable data quality, removing conflicts between the data and known constraints, and increasing adherence to the properties required by the proposed models. Preprocessing methods can analyze past decisions, identify conflicting observations and criteria, and prompt the decision-maker to either remove or rectify any mismatch in the past data. This pre-processing results in data that is well-defined for the FO problem. If the data is still ill-posed, we will need to extend the model to allow inconsistencies in the data, as discussed next.

6.2. Ill-posed Data

In Section 2, we assumed that the data is well-posed and there are no inconsistencies in the observations, particularly, $\{ \exists k \in \mathcal{K}^- | \mathbf{x}^k \in \mathcal{H} \}$, indicating that there are no rejected observations in the convex hull of accepted observations as captured by Assumption 1. In practical settings, however, this assumption may be violated due to data inconsistency. Data pre-processing can capture and correct some of such inconsistencies, as discussed in Section 6.1. Another approach is to modify the RGIO model to introduce a regularization term that penalizes a slack that captures the violation in the inferred constraints to the loss function of the inverse problem. This addition will change the nature of the inferred constraints from hard constraints to soft constraints that allow violations with a certain penalty. In the context of our proposed RGIO model, this can be achieved via the following model RGIO- ξ .

$$\text{Maximize}_{\mathbf{a}, \mathbf{b}, \mathbf{q}, \mathbf{y}} \quad \mathcal{D}(\mathbf{q}_1, \dots, \mathbf{q}_{|\tilde{\mathcal{N}}|}, \mathbf{A}, \mathbf{b}; (\mathbf{x}^1, \dots, \mathbf{x}^{|\mathcal{K}^+|})) - \mathcal{D}_\xi(\xi^{\mathcal{L}^+}, \xi^{\mathcal{L}^-}, \xi^{\mathcal{N}^+}, \xi^{\mathcal{N}^-}) \quad (8a)$$

$$\text{subject to} \quad g_n(\mathbf{x}^k; \mathbf{q}_n) \geq -\xi_{n,k}^{\mathcal{N}^+}, \quad \forall k \in \mathcal{K}^+, n \in \tilde{\mathcal{N}} \quad (8b)$$

$$\mathbf{a}'_\ell \mathbf{x}^k - b_\ell \geq -\xi_{\ell,k}^{\mathcal{L}^+}, \quad \forall k \in \mathcal{K}^+, \ell \in \tilde{\mathcal{L}} \quad (8c)$$

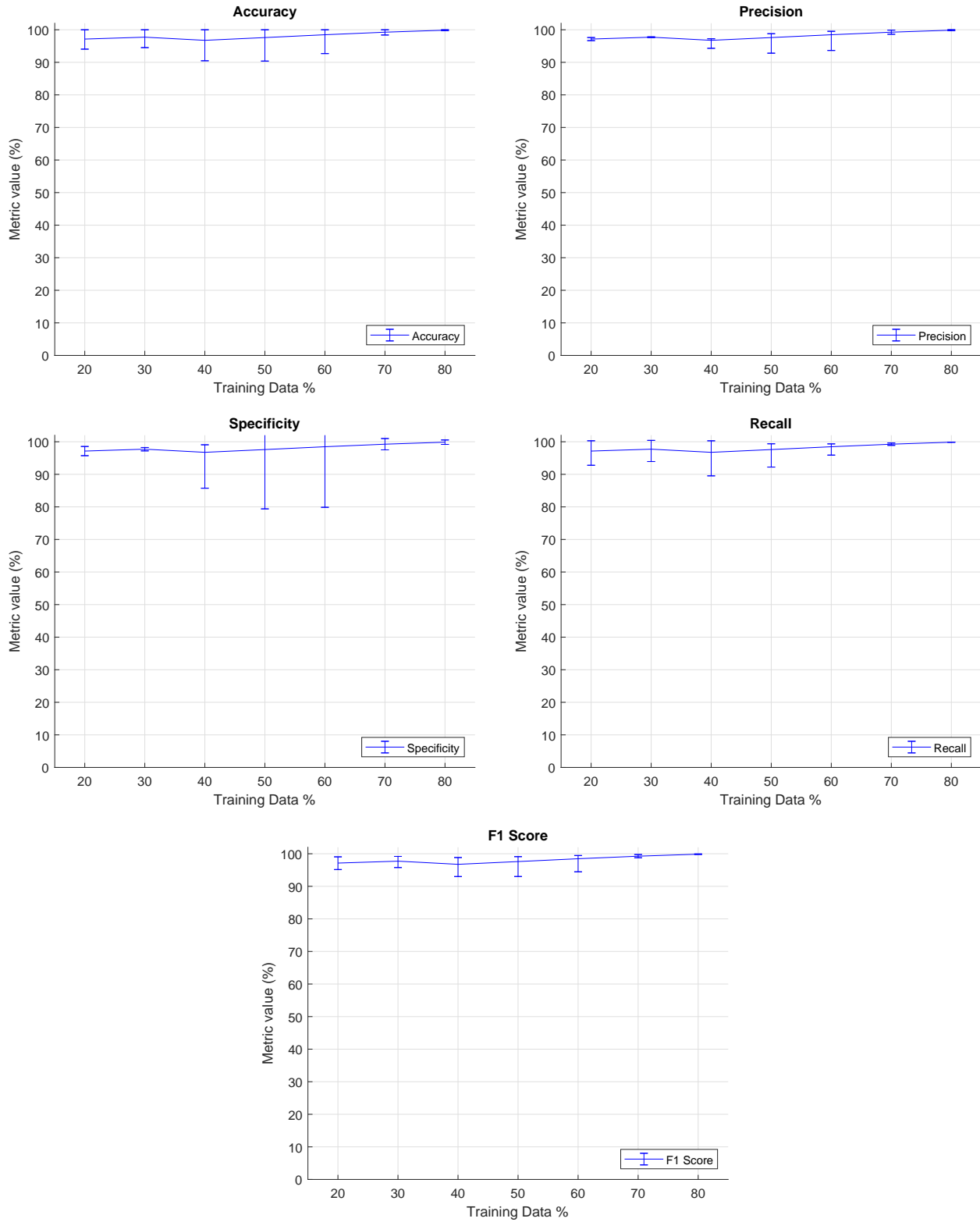


Figure 11 Sensitivity of different metrics with respect to the proportion of past/future patients

$$g_n(\mathbf{x}^k; \mathbf{q}_n) + \epsilon - My_{nk} \leq \xi_{n,k}^{N-}, \quad \forall n \in \mathcal{N} \cup \tilde{\mathcal{N}}, k \in \mathcal{K}^- \quad (8d)$$

$$\mathbf{a}_\ell \mathbf{x}^k - b_\ell + \epsilon - My_{\ell k} \leq \xi_{\ell,k}^{L-}, \quad \forall \ell \in \mathcal{L} \cup \tilde{\mathcal{L}}, k \in \mathcal{K}^- \quad (8e)$$

$$\xi^{\mathcal{L}+}, \xi^{\mathcal{L}-}, \xi^{\mathcal{N}+}, \xi^{\mathcal{N}-} \geq \mathbf{0}, \quad (8f)$$

$$(3f) - (3i).$$

6.3. Data Uncertainty

An area of future research is to consider the effect of data uncertainty on constraint inference and to explore robustness conditions for the inverse framework. In the literature on inverse for objective inference, robust optimization has been used to tackle data uncertainty where an uncertainty set is considered around each data input (Ghobadi et al. 2018). A similar approach can be used for constraint inference, where uncertainty sets are considered around both the accepted and rejected observations and the goal of the inverse model is to infer a feasible region that is robust against the worst-case scenario of data uncertainty. We note that these uncertainty sets may overlap, which may necessitate the use of soft margins and a notion of error as discussed in Section 6.2.

6.4. Overfitting

Depending on the loss function used in our proposed inverse framework, it is possible to overfit to the data by either inferring a feasible region that is tightly wrapped around the accepted observation and disallowing other potentially acceptable solutions that are just outside this region, or on the contrary, inferring a loose feasible region that only eliminates past rejected solutions. An intuitive method to avoid overfitting is to consider a margin around observations, which would be mathematically similar to considering an uncertainty set around each observation, as discussed in Section 6.3. Another possible direction is to define a measure of optimism (or pessimism) which indicates how much to expand the feasible region to allow better solution (or contract the region to deviate from the rejected data). In combination with the methods from Section 6.2, this tunable parameter would allow the user to decide how conservative they want to be concerning overfitting to both the accepted and the rejected past data.

6.5. Benchmarking

We note that although this work conveys some similarities with classification methods, it is structurally different from the conventional artificial intelligence classification, e.g., support vector machines. Inferring a feasible region has connections with binary classification methods, distinguishing between the interior and exterior of the feasible region. While traditional classification methods often include assumptions on the type of separators, they rarely consider any assumptions on the recovered region or objective functions. In this work, we include the explicit setting where the inferred feasible region must be a convex set so that it can later be used in a forward convex optimization setting. This connection can be further explored between existing classification methods and inverse optimization, investigating distance measures that can be used and the properties of the obtained region. Future work can also explore the relationship between the distribution of observations and the inferred feasible region.

7. Conclusions

In summary, this paper provides an inverse optimization framework that inputs both accepted and rejected observations and imputes a convex feasible region of a forward problem. The proposed inverse model is a complex nonlinear mixed integer formulation; therefore, using the properties of the constructed solutions, we propose a reduced reformulation that partially mitigates the problem complexity by using variational inequalities to render a set of nonlinear optimality conditions redundant.

We consider the problem of radiation therapy treatment planning to infer the implicit clinical guidelines that are utilized in practice based on historical plans. Using realistic patient datasets, we randomly divide the data into past and future patients and use our inverse models to derive a feasible region for accepted

plans such that rejected plans are infeasible. Our results show that on average, 98% of the plans that are feasible for our inferred models are also historically accepted, and our obtained feasible region (i.e., the underlying clinical guidelines) performs with 95% accuracy in predicting the accepted and rejected treatment plans for future patients, on average. The results also highlight an interesting property of IO models: even with a small size of past patient data, a high accuracy can be obtained in generating acceptable plans for future patients. This characteristic, perhaps one of the advantages of IO compared to conventional machine learning methods, is due to the fact that IO models have a predetermined optimization structure.

In radiation therapy, implementing our methodology results in standardized clinical guidelines and infers the true underlying criteria based on which the accept/reject decisions are made. This information allows planners to generate higher-quality initial plans that, in turn, result in better patient care through personalized treatment plans. It also streamlines the planning process by reducing the number of times a plan is rejected and sent back for corrections. The standardization of the guidelines reduces variability and potential human errors among clinicians and health care centers, and enables personalized guidelines for patient subpopulations. We believe the method can also be applied in other application areas where an understanding of implicit expert constraints can help streamline the decision-making processes. One future direction consists of focusing on special classes of convex problems and devising more efficient solution methods for large-case data-driven applications.

References

- Ahmadi F, Dai T, Ghobadi K (2022) You are what you eat: A preference-aware inverse optimization approach. *arXiv preprint arXiv:2212.05201* .
- Ahmadi F, Ganjkanloo F, Ghobadi K (2020) Inverse learning: A data-driven framework to infer optimizations models. *arXiv preprint arXiv:2011.03038* .
- Ahuja RK, Orlin JB (2001) Inverse optimization. *Operations Research* 49(5):771–783.
- Ajayi T, Lee T, Schaefer AJ (2022) Objective selection for cancer treatment: an inverse optimization approach. *Operations Research* .
- American Cancer Society (2023) Cancer Statistics Center. <http://cancerstatisticscenter.cancer.org> [Accessed: 04.10.2023].
- Aswani A, Shen ZJ, Siddiq A (2018) Inverse optimization with noisy data. *Operations Research* 66(3):870–892.
- Aswani A, Shen ZJM, A (2019) Data-driven incentive design in the medicare shared savings program. *Operations Research* 67(4):1002–1026.
- Babier A, Boutilier JJ, Sharpe MB, McNiven AL, Chan TC (2018) Inverse optimization of objective function weights for treatment planning using clinical dose-volume histograms. *Physics in Medicine & Biology* 63(10):105004.
- Babier A, Chan TC, Lee T, Mahmood R, Terekhov D (2021) An ensemble learning framework for model fitting and evaluation in inverse linear optimization. *Informatics Journal on Optimization* 3(2):119–138.
- Babier A, Mahmood R, McNiven AL, Diamant A, Chan TC (2020) Knowledge-based automated planning with three-dimensional generative adversarial networks. *Medical Physics* 47(2):297–306.
- Bertsimas D, Gupta V, Paschalidis IC (2015a) Data-driven estimation in equilibrium using inverse optimization. *Mathematical Programming* 153(2):595–633.
- Bertsimas D, Gupta V, Paschalidis IC (2015b) Data-driven estimation in equilibrium using inverse optimization. *Mathematical Programming* 153:595–633.
- Birge JR, Hortaçsu A, Pavlin JM (2017) Inverse optimization for the recovery of market structure from market outcomes: An application to the MISO electricity market. *Operations Research* 65(4):837–855.
- Boutilier JJ, Lee T, Craig T, Sharpe MB, Chan TC (2015) Models for predicting objective function weights in prostate cancer imrt. *Medical physics* 42(4):1586–1595.
- Boyd S, Vandenberghe L (2004) *Convex optimization* (Cambridge university press).
- Brucker P, Shakhlevich NV (2009) Inverse scheduling with maximum lateness objective. *Journal of Scheduling* 12(5):475–488.

- Černý M, Hladík M (2016) Inverse optimization: towards the optimal parameter set of inverse LP with interval coefficients. *Central European Journal of Operations Research* 24(3):747–762.
- Chan TC, Eberg M, Forster K, Holloway C, Ieraci L, Shalaby Y, Yousefi N (2022) An inverse optimization approach to measuring clinical pathway concordance. *Management Science* 68(3):1882–1903.
- Chan TC, Kaw N (2020) Inverse optimization for the recovery of constraint parameters. *European Journal of Operational Research* 282(2):415–427.
- Chan TC, Lee T (2018) Trade-off preservation in inverse multi-objective convex optimization. *European Journal of Operational Research* 270(1):25–39.
- Chan TC, Lee T, Terekhov D (2019) Inverse optimization: Closed-form solutions, geometry, and goodness of fit. *Management Science* 65(3):1115–1135.
- Chan TC, Mahmood R, Zhu IY (2023) Inverse optimization: Theory and applications. *Operations Research* .
- Chan TC, Mahmoudzadeh H, Purdie TG (2014a) A robust-cvar optimization approach with application to breast cancer therapy. *European Journal of Operational Research* 238(3):876–885.
- Chan TCY, Craig T, Lee T, Sharpe MB (2014b) Generalized inverse multi-objective optimization with application to cancer therapy. *Operations Research* 62(3):680–695.
- Chow JYJ, Recker WW (2012) Inverse optimization with endogenous arrival time constraints to calibrate the household activity pattern problem. *Transportation Research Part B: Methodological* 46(3):463–479.
- Dempe S, Lohse S (2006) Inverse linear programming. *Recent Advances in Optimization*, 19–28 (Springer).
- Esfahani PM, Shafieezadeh-Abadeh S, Hanasusanto GA, Kuhn D (2018) Data-driven inverse optimization with incomplete information. *Mathematical Programming* 167(1):191–234.
- Fernández-Blanco R, Morales JM, Pineda S (2021) Forecasting the price-response of a pool of buildings via homothetic inverse optimization. *Applied Energy* 290:116791.
- Gebken B, Peitz S (2021) Inverse multiobjective optimization: Inferring decision criteria from data. *Journal of Global Optimization* 80(1):3–29.
- Ghate A (2020a) Imputing radiobiological parameters of the linear-quadratic dose-response model from a radiotherapy fractionation plan. *Physics in Medicine & Biology* 65(22):225009.
- Ghate A (2020b) Inverse optimization in semi-infinite linear programs. *Operations Research Letters* 48(3):278–285.
- Ghatrani Z, Ghate A (2022) Inverse markov decision processes with unknown transition probabilities. *IISE Transactions* 1–14.
- Ghatrani Z, Ghate A (2024) Inverse optimization in semi-definite programs to impute unknown constraint matrices. *Computers & Operations Research* 168:106681.
- Ghobadi K (2014) *Optimization methods for patient positioning in Leksell Gamma Knife Perfexion*. Ph.D. thesis, University of Toronto.
- Ghobadi K, Lee T, Mahmoudzadeh H, Terekhov D (2018) Robust inverse optimization. *Operations Research Letters* 46(3):339–344.
- Ghobadi K, Mahmoudzadeh H (2021) Inferring linear feasible regions using inverse optimization. *European Journal of Operational Research* 290(3):829–843.
- Goli A, Boutilier JJ, Craig T, Sharpe MB, Chan TC (2018) A small number of objective function weight vectors is sufficient for automated treatment planning in prostate cancer. *Physics in Medicine & Biology* 63(19):195004.
- Güler Ç, Hamacher HW (2010) Capacity inverse minimum cost flow problem. *Journal of Combinatorial Optimization* 19(1):43–59.
- Gupta R, Zhang Q (2023) Efficient learning of decision-making models: A penalty block coordinate descent algorithm for data-driven inverse optimization. *Computers & Chemical Engineering* 170:108123.
- Harker PT, Pang JS (1990) Finite-dimensional variational inequality and nonlinear complementarity problems: a survey of theory, algorithms and applications. *Mathematical programming* 48(1-3):161–220.
- Iyengar G, Kang W (2005) Inverse conic programming with applications. *Operations Research Letters* 33(3):319–330.

- Keshavarz A, Wang Y, Boyd S (2011) Imputing a convex objective function. *2011 IEEE International Symposium on Intelligent Control (ISIC)*, 613–619 (IEEE).
- Kinderlehrer D, Stampacchia G (2000) *An introduction to variational inequalities and their applications* (SIAM).
- Lee T, Hammad M, Chan TC, Craig T, Sharpe MB (2013) Predicting objective function weights from patient anatomy in prostate imrt treatment planning. *Medical physics* 40(12):121706.
- Li JYM (2021) Inverse optimization of convex risk functions. *Management Science* 67(11):7113–7141.
- Mahmoudzadeh H, Lee J, Chan TC, Purdie TG (2015) Robust optimization methods for cardiac sparing in tangential breast imrt. *Medical physics* 42(5):2212–2222.
- Naghavi M, Foroughi AA, Zarepisheh M (2019) Inverse optimization for multi-objective linear programming. *Optimization Letters* 13(2):281–294.
- Roland J, Figueira JR, De Smet Y (2016) Finding compromise solutions in project portfolio selection with multiple experts by inverse optimization. *Computers & Operations Research* 66:12–19.
- Saez-Gallego J, Morales JM (2018) Short-term forecasting of price-responsive loads using inverse optimization. *IEEE Transactions on Smart Grid* 9(5):4805–4814.
- Sayre G, Ruan D (2014) Automatic treatment planning with convex imputing. *Journal of Physics: Conference Series*, volume 489, 012058 (IOP Publishing).
- Shahmoradi Z, Lee T (2021) Quantile inverse optimization: Improving stability in inverse linear programming. *Operations Research* .
- Shahmoradi Z, Lee T (2022) Optimality-based clustering: An inverse optimization approach. *Operations Research Letters* 50(2):205–212, ISSN 0167-6377, URL <http://dx.doi.org/https://doi.org/10.1016/j.orl.2021.12.012>.
- Tavaslıoğlu O, Lee T, Valeva S, Schaefer AJ (2018) On the structure of the inverse-feasible region of a linear program. *Operations Research Letters* 46(1):147–152.
- Troutt MD, Brandyberry AA, Sohn C, Tadisina SK (2008) Linear programming system identification: The general nonnegative parameters case. *European Journal of Operational Research* 185(1):63–75.
- Troutt MD, Pang WK, Hou SH (2006) Behavioral estimation of mathematical programming objective function coefficients. *Management Science* 52(3):422–434.
- Wong JW, Sharpe MB, Jaffray DA, Kini VR, Robertson JM, Stromberg JS, Martinez AA (1999) The use of active breathing control (abc) to reduce margin for breathing motion. *International Journal of Radiation Oncology* Biology* Physics* 44(4):911–919.
- Yu S, Wang H, Dong C (2023) Learning risk preferences from investment portfolios using inverse optimization. *Research in International Business and Finance* 101879.
- Zhang J, Liu Z (1999) A further study on inverse linear programming problems. *Journal of Computational and Applied Mathematics* 106(2):345–359.
- Zhang J, Xu C (2010) Inverse optimization for linearly constrained convex separable programming problems. *European Journal of Operational Research* 200(3):671–679.
- Zhang J, Zhang L (2010) An augmented lagrangian method for a class of inverse quadratic programming problems. *Applied Mathematics and Optimization* 61(1):57–83.

Appendix A: Proofs

PROOF OF PROPOSITION 1. Constraints (2b)–(2c) ensure $\mathbf{x}^k \in \tilde{\mathcal{X}}, \forall k \in \mathcal{K}$, and constraints (2g)–(2i) use binary variables y_{ik} to ensure that at least one constraint (either inferred or known; linear or nonlinear) makes each rejected point infeasible, which, in turn, ensures $\mathbf{x}^k \notin \mathcal{X} \cap \tilde{\mathcal{X}}$. Therefore, the conditions of Definition 2 are met and \mathcal{X} is a nominal set. Since the set $\tilde{\mathcal{X}} \cap \mathcal{X}$ is convex by definition, constraints (2b)–(2f) provide the necessary and sufficient KKT conditions to guarantee $\mathbf{x}^0 \in \arg \min_{\mathbf{x} \in \mathcal{X} \cap \tilde{\mathcal{X}}} \{f(\mathbf{x}; \mathbf{c})\}$. \square

PROOF OF PROPOSITION 2. To show that the feasible region is non-empty, we construct a solution (by assigning values to all variables $\mathbf{q}, \mathbf{a}, b, \lambda, \mu$, and y) that satisfies all constraints of GIO and is, hence, feasible. Let $\mathbf{q}_n = \hat{\mathbf{q}}, \forall n \in \tilde{\mathcal{N}}$, as defined in Assumption 1. By Assumption 1 and the Separating Hyperplane Theorem (Boyd and Vandenberghe 2004), for every rejected point $k \in \mathcal{K}^-, \exists \hat{\mathbf{a}}_k, \hat{b}_k$ such that $\hat{\mathbf{a}}_k' \mathbf{x}^k < \hat{b}_k$ and $\hat{\mathbf{a}}_k' \mathbf{x}^p \geq \hat{b}_k, \forall p \in \mathcal{K}^+$. Let $[\mathbf{a}_\ell] = [\hat{\mathbf{a}}_1, \dots, \hat{\mathbf{a}}_{|\mathcal{K}^-|}, \nabla f(\mathbf{x}^0; \mathbf{c}), \dots, \nabla f(\mathbf{x}^0; \mathbf{c})]$ and $\mathbf{b} = [\hat{b}_1, \dots, \hat{b}_{|\mathcal{K}^-|}, \nabla(\mathbf{x}^0; \mathbf{c})' \mathbf{x}^0, \dots, \nabla(\mathbf{x}^0; \mathbf{c})' \mathbf{x}^0], \forall \ell \in \{1, \dots, \mathcal{L}\}$. Let the dual variables of the nonlinear and linear constraints be $\lambda_n = 0, \forall n \in \mathcal{N} \cup \tilde{\mathcal{N}}$, and $[\mu_\ell] = [\mathbf{0}_{1 \times |\mathcal{L} \cup \tilde{\mathcal{L}}| - 1}, -1], \forall \ell \in \mathcal{L}$, respectively. Finally, let binary variables $y_{kk} = 0, \forall i \in \tilde{\mathcal{L}}, k \in \mathcal{K}^-$ and $y_{kk} = 1, \forall i \in \mathcal{I} \setminus \tilde{\mathcal{L}}, k \in \mathcal{K}^-$. By substitution, it can be seen that this constructed solution satisfies all constraints (2c)–(2m). Note that the first $|\mathcal{K}^-|$ constraints ensure that each rejected point is infeasible for at least one inferred linear constraint, and the last set of constraints (which are all identical) ensure the optimality of \mathbf{x}^0 . All constraints satisfy primal feasibility $\forall \mathbf{x}^k, k \in \mathcal{K}^+$. \square

PROOF OF PROPOSITION 3. Let $\mathcal{S} = \mathcal{X} \cap \tilde{\mathcal{X}}$ be an imputed set for FO. Assume that $\mathcal{S} \not\subseteq \mathcal{C}$. Then $\exists \hat{\mathbf{x}} \in \mathcal{S} \setminus \mathcal{C}$. We know that $\hat{\mathbf{x}} \notin \mathcal{V}$ since it contradicts the definition of the preferred solution \mathbf{x}^0 . Hence, $\hat{\mathbf{x}} \in \mathcal{V} \setminus \mathcal{C}$. Consider the following two cases:

Case 1: If $f(\mathbf{x}; \mathbf{c})$ is linear, then $\mathcal{C} = \mathcal{V}$ and $\mathcal{V} \setminus \mathcal{C} = \emptyset$, which is in contradiction with $\mathbf{x}^k \in \mathcal{V} \setminus \mathcal{C}$.

Case 2: If $f(\mathbf{x}; \mathbf{c})$ is nonlinear convex, then \mathcal{V} is non-convex, and hence $\mathcal{V} \setminus \mathcal{C}$ is non-convex. Given that \mathcal{C} is the tangent half-space of the sublevel set of $f(\mathbf{x}; \mathbf{c})$ at \mathbf{x}^0 , then \mathbf{x}^0 is on the boundary of \mathcal{V} since f is monotone. Because \mathcal{S} is convex, for any $\hat{\mathbf{x}} \in \mathcal{V} \setminus \mathcal{C}$, there must exist $\lambda > 0$ such that $\bar{\mathbf{x}} = \lambda \hat{\mathbf{x}} + (1 - \lambda) \mathbf{x}^0$ and $\bar{\mathbf{x}} \in \mathcal{S} \setminus \mathcal{V}$, which contradicts $\mathbf{x}^0 \in \arg \min_{\mathbf{x} \in \mathcal{S}} \{f(\mathbf{x}; \mathbf{c})\}$. \square

PROOF OF PROPOSITION 4. Both \mathcal{S} and \mathcal{C} are convex so $\mathcal{C} \cap \mathcal{S}$ is also convex. Because \mathcal{S} is a nominal set and \mathcal{C} includes all accepted observations, $\mathcal{C} \cap \mathcal{S}$ is also a convex nominal set. Finally, Since \mathcal{S} is a convex nominal set, it includes the convex hull of all observations, and $\mathbf{x}^0 \in \mathcal{S}$, and therefore, $\mathbf{x}^0 \in \mathcal{S} \cap \mathcal{C}$. Because \mathcal{C} is the tangent half-space to the sublevel set of $f(\mathbf{x}; \mathbf{c})$ at \mathbf{x}^0 , it is also given that $\mathbf{x}^0 \in \arg \min_{\mathbf{x} \in \mathcal{S} \cap \mathcal{C}} \{f(\mathbf{x}; \mathbf{c})\}$. Therefore, $\mathcal{S} \cap \mathcal{C}$ meets the criteria outlined in Definition 5 and is, therefore, an imputed set.

PROOF OF THEOREM 1. (i) Any solution $\mathbf{a}, b, \mathbf{q}, \lambda, \mu, y$ of GIO is also a solution of RGIO because it has fewer constraints. (ii) Vice-versa, for any solution $\mathbf{a}, b, \mathbf{q}, y$ of RGIO there exists a solution of GIO since \mathcal{C} is appended to the known constraints and the stationarity and complementary slackness conditions can be re-written as:

$$\begin{aligned} \nabla f(\mathbf{x}^0; \mathbf{c}) + \sum_{n \in \mathcal{N} \cup \tilde{\mathcal{N}}} \lambda_n \nabla g_n(\mathbf{x}^0, \mathbf{q}_n) + \lambda_0 \nabla f(\mathbf{x}^0; \mathbf{c}) + \sum_{\ell \in \mathcal{L} \cup \tilde{\mathcal{L}}} \mu_\ell \mathbf{a}_\ell &= \mathbf{0} \\ \lambda_0 (\nabla f(\mathbf{x}^0; \mathbf{c})' \mathbf{x}^0 - \nabla f(\mathbf{x}^0; \mathbf{c})' \mathbf{x}^0) &= 0 \\ \lambda_n g_n(\mathbf{x}^0, \mathbf{q}_n) &= 0 \quad \forall n \in \mathcal{N} \cup \tilde{\mathcal{N}}, \\ \mu_\ell (b_\ell - \mathbf{a}'_\ell \mathbf{x}^0) &= 0, \quad \forall \ell \in \mathcal{L} \cup \tilde{\mathcal{L}} \\ \lambda_n, \mu_\ell &\leq 0, \quad \forall n \in \mathcal{N} \cup \tilde{\mathcal{N}}, \ell \in \mathcal{L} \cup \tilde{\mathcal{L}}. \end{aligned}$$

All conditions are satisfied if we set $\lambda_0 = -1$ and $\lambda_n, \mu_\ell \leq 0, \forall n \in \mathcal{N} \cup \tilde{\mathcal{N}}, \ell \in \mathcal{L} \cup \tilde{\mathcal{L}}$. Hence, for any solution to RGIO, there exists a corresponding solution to GIO. Therefore, by (i) and (ii), the GIO and RGIO are equivalent when \mathcal{C} is added as a known constraint. \square

PROOF OF COROLLARY 1. Due to constraints (3b)–(3i), we know that $\tilde{\mathcal{X}}$ is a nominal feasible set for FO. Note that $\mathbf{x}^0 \in \mathcal{X} \cap \tilde{\mathcal{X}} \cap \mathcal{C}$ given that $\mathbf{x}^0 \in \mathcal{X}$ by Assumption 1, $\mathbf{x}^0 \in \tilde{\mathcal{X}}$ because $\tilde{\mathcal{X}}$ is a nominal set, and $\mathbf{x}^0 \in \mathcal{C}$ by definition.

Furthermore, $\mathbf{x}^0 \in \mathcal{C} = \{\mathbf{x} \mid f(\mathbf{x}; \mathbf{c}) \geq f(\mathbf{x}^0; \mathbf{c})\}$, which implies that $\mathbf{x}^0 \in \arg \min_{\mathbf{x} \in \mathcal{C} \cap \mathcal{X} \cap \tilde{\mathcal{X}}} f(\mathbf{x}; \mathbf{c})$ and is therefore an optimal solution of (4a). \square

Appendix B: Forward and Inverse Models for the Radiation Therapy Application

Assume that a set of features $f \in \mathcal{F}$ is given for each structure $s \in \mathcal{S}$, for instance left lung, clinical target volume (CTV), and the heart for a breast cancer patient. Examples of the features in radiation therapy plans for such patients include min, max, mean dose, or dose to a certain volume of each structure. The Forward problem we consider is a linear optimization in which the objective function is a linear measure of the features, i.e., \mathbf{x} which is a vector of x_i where $i \in I_1$ and I_1 is the vector of all dosimetric features of the plans. The ordered list of these dosimetric features is provided in Figure 9. Accordingly, the forward problem for the RT problem can be written as

$$\begin{aligned} \text{FO: Minimize} \quad & \mathbf{c}'\mathbf{x} & (9) \\ \text{subject to} \quad & \mathbf{G}\mathbf{x} \geq \mathbf{h} & \text{(Known constraints)} \\ & \mathbf{A}\mathbf{x} \geq \mathbf{b}, & \text{(Unknown constraints)} \end{aligned}$$

where, $\mathbf{G} = \mathbf{I}_{14 \times 14}$ is the identity matrix, $\mathbf{h} = [10, \mathbf{0}_{1 \times 13}]'$ to ensure the minimum dose to every voxel in the clinical target volume is always at least 10 Gy and the dose to all other structures are always non-negative. The objective function coefficient vector is $\mathbf{c} = [0 \ 0 \ 0 \ 0 \ 0 \ 0 \ 0 \ 0 \ 0 \ 1 \ 1 \ 0 \ 0 \ 0]'$ to minimize the max dose to the organs at risk, namely the heart and the left lung. In this model, we aim to recover 10 unknown underlying constraints using inverse optimization, and hence, the matrix \mathbf{A} and vector \mathbf{b} are the unknown parameters of sizes 10×14 and 10×1 , respectively, which will be inferred in the inverse model. Using the Separation Metric, and based on formulation (5), the resulting inverse model is a mixed integer linear program and can be written as follows.

$$\text{Maximize}_{\mathbf{a}, \mathbf{b}, \mathbf{p}, \mathbf{y}, \mathbf{z}} \quad \sum_{k \in \mathcal{K}^-} z_k \quad (10a)$$

$$\text{subject to} \quad d_{\ell k} \geq b_\ell - \mathbf{a}'_\ell \mathbf{x}^k, \quad \forall \ell \in \tilde{\mathcal{L}}, k \in \mathcal{K}^- \quad (10b)$$

$$d_{\ell k} \leq b_\ell - \mathbf{a}'_\ell \mathbf{x}^k + M y_{\ell k}, \quad \forall \ell \in \tilde{\mathcal{L}}, k \in \mathcal{K}^- \quad (10c)$$

$$d_{\ell k} \leq M(1 - y_{\ell k}), \quad \forall \ell \in \tilde{\mathcal{L}}, k \in \mathcal{K}^- \quad (10d)$$

$$d_{\ell k} \geq \epsilon(1 - y_{\ell k}), \quad \forall \ell \in \tilde{\mathcal{L}}, k \in \mathcal{K}^- \quad (10e)$$

$$z_k \leq d_{\ell k} + M p_{\ell k}, \quad \forall \ell \in \tilde{\mathcal{L}}, k \in \mathcal{K}^- \quad (10f)$$

$$\sum_{\ell \in \tilde{\mathcal{L}}} p_{\ell k} \leq |\tilde{\mathcal{L}}| - 1, \quad \forall k \in \mathcal{K}^- \quad (10g)$$

$$p_{\ell k} \geq y_{\ell k}, \quad \forall \ell \in \tilde{\mathcal{L}}, k \in \mathcal{K}^- \quad (10h)$$

$$d_{\ell k} \geq 0, \quad \forall \ell \in \tilde{\mathcal{L}}, k \in \mathcal{K}^- \quad (10i)$$

$$\mathbf{a}'_\ell \mathbf{x}^k \geq b_\ell, \quad \forall k \in \mathcal{K}^+, \ell \in \tilde{\mathcal{L}} \quad (10j)$$

$$\mathbf{a}_\ell \mathbf{x}^k \leq b_\ell - \epsilon + M y_{\ell k}, \quad \forall \ell \in \tilde{\mathcal{L}}, k \in \mathcal{K}^- \quad (10k)$$

$$\sum_{\ell \in \tilde{\mathcal{L}}} y_{\ell k} \leq |\tilde{\mathcal{L}}| - 1, \quad \forall k \in \mathcal{K}^- \quad (10l)$$

$$\sum_{j=1}^m a_{\ell j} = \alpha_\ell^+ - \alpha_\ell^- \quad (10m)$$

$$\alpha_\ell^+ + \alpha_\ell^- = 1 \quad (10n)$$

$$y_{\ell k}, \alpha_\ell^-, \alpha_\ell^- \in \{0, 1\}, \quad \forall \ell \in \tilde{\mathcal{L}}, k \in \mathcal{K}^- \quad (10o)$$

$$\mathbf{a}_\ell \in \mathbb{R}^m, b_\ell \in \mathbb{R}, \quad \forall \ell \in \tilde{\mathcal{L}}. \quad (10p)$$

In this model, to normalize the left-hand-side parameters of the inferred constraints, we use a linear proxy to the L_1 norm from Ghobadi and Mahmoudzadeh (2021) as shown in constraints (10m)-(10n).